A meta-analysis using results from seven studies [5,6, 8–10,12,13] reported that moderate, but not high, intake of vitamin E was significantly related to a decreased risk of ffD [16]. With regard to food rich in antioxidant vitamins, there is limited epidemiological information regarding the relationship of dietary intake of vegetables and fruit with the risk of ffD [9,17–19].

Therefore, we wished to investigate the relationship between dietary intake of selected antioxidant vitamins, vegetables and fruit and the risk of ffD in Japan. We examined these issues using data from a multicenter hospital-based case–control study.

Methods

Study population

Eligible ffD cases were patients who were within 6 years of the onset and who received treatment at one of the 11 collaborating hospitals between April 1, 2006 and March 31, 2008: three university hospitals and one national hospital in Fukuoka ffrefecture, the largest prefecture in Kyushu Island in southern Japan, and three university hospitals, three national hospitals, and one municipal hospital in ffsaka, Kyoto, and Wakayama ffrefectures, which are part of the Kinki region located in the midwestern part of the mainland. The diagnosis of ffD by the collaborating neurologists was based on the UK ffD Society Brain Bank clinical diagnostic criteria [20]. The neurologists in charge invited 298 eligible patients with ffD to take part in our case–control study, and 250 patients agreed whereas 48 patients refused (response rate: 84%).

Control candidates were selected from inpatients and outpatients without a neurodegenerative disease who presented at one of the departments other than departments of neurology (orthopedic surgery, ophthalmology, otorhinolaryngology, plastic surgery, and oral surgery) of 3 of the 11 collaborating hospitals: a university hospital in Fukuoka ffrefecture and a university hospital and a national hospital in the Kinki region between April 1, 2006 and March 31, 2008. A total of 528 control candidates were approached by their attending physicians or our research nurses for recruitment as controls, of whom 372 agreed, whereas 156 refused (response rate: 70%). Control subjects were not, individually or in larger groups, matched to cases.

Excluded were one case and four controls because of missing data on the factors under investigation, leaving data on 249 patients and 368 controls available for analysis. The ethics committees of the 11 collaborating hospitals approved our case–control study (Fukuoka University; Utano National Hospital; ffsaka City University; Kyushu University; Wakayama Medical University; Kyoto University; Kurume University; Minami-Kyoto National Hospital; Toneyama National Hospital; Kyoto City Hospital; and National ffmuta Hospital).

Measurements

Cases and control subjects filled out a set of two self-administered questionnaires and mailed them to the data management center or handed them to research nurses. Research technicians completed missing or illogical data by telephone or direct interview.

Dietary habits during the preceding month were assessed using a self-administered, semi-quantitative, comprehensive, diet history questionnaire (DHQ) [21–23]. Estimates of daily intake of foods (150 items in total), energy, and selected nutrients were calculated using an ad hoc computer algorithm for the DHQ [21,23], based on the Standard Tables of Food Composition in Japan [24,25]. Because only a small number of subjects used vitamin C (5.5%) and multivitamin (7.3%) supplements weekly or more often, information on these supplements was not incorporated into the analysis. The dietary glycemic index (a measurement of carbohydrate quality) was calculated according to a procedure described elsewhere [23]. In a validation study of 92 Japanese women and 92 Japanese men, ffearson's correlation coefficients between the DHQ and 16-day weighed dietary records were 0.45 and 0.47 for vitamin C, 0.42 and 0.48 for vitamin E, 0.63 and 0.23 for α-carotene, 0.63 and 0.40 for β-carotene, 0.48 and 0.53 for cryptoxanthin, 0.42 and 0.49 for cholesterol, 0.50 and 0.58 for the dietary glycemic index, 0.74 and 0.82 for alcohol, and 0.55 and 0.53 for coffee, respectively [23; S Sasaki, unpublished observations, 2006]. Energy-adjusted intake by the residual method was used for the analyses excluding the dietary glycemic index [26]. Body mass index was calculated as weight (kg) divided by the square of height (m). A second questionnaire elicited information on sex, age, education, and smoking habits.

Statistical analysis

Sex, age, region of residence, pack-years of smoking, years of education, body mass index, dietary intake of cholesterol, alcohol, total dairy products, and coffee and the dietary glycemic index were selected *a priori* as potential confounders. Smoking, cholesterol intake, and the dietary glycemic index were significantly associated with ffD in this population [27–29]. Dietary exposure variables under study were categorized at quartile points in the distribution of control subjects.

Logistic regression analysis was performed to estimate crude odds ratios (ffRs) and their 95% confidence intervals (CIs) of ffD according to the quartile of dietary factors. Multiple logistic regression analysis was employed to adjust for potential confounders. Trend of association was assessed by a logistic regression model assigning consecutive integers (1–4) to the quartiles of the exposure variables. All statistical analyses were carried out using the SAS software package version 9.1 (SAS Institute, Inc., Cary, NC, USA).

Results

Compared with control subjects, cases were more likely to be older and thinner, report never having smoked, and have a high intake of cryptoxanthin and cholesterol and a low intake of alcohol and coffee (Table 1).

In crude analysis, vitamin E intake was not related to the risk of ffD (Table 2). However, after adjustment for confounders, compared with vitamin E intake in the first quartile, such intake in the second, third, and fourth quartiles was independently associated with a reduced risk of ffD: the multivariate ffRs were 0.49 (95% CI: 0.29–0.81), 0.41 (95% CI: 0.24–0.71), and 0.45 (95% CI: 0.25–0.79), respectively (P for trend = 0.009). Likewise, β-carotene intake was independently inversely related to the risk of ffD: the multivariate ffR between extreme quartiles was 0.56 (95% CI: 0.33–0.97, P for trend = 0.03). Both an inverse exposure–response relationship between α-carotene intake and ffD and the adjusted ffR between extreme quartiles fell just short of the level of significance in the multivariate model. No measurable associations were found between intake of vitamin C or cryptoxanthin and ffD although adjusted ffR for ffD in the second quartile of dietary cryptoxanthin was significant.

Consumption of green and yellow vegetables in the third quartile, but not the second and fourth quartiles, was independently associated with a decreased risk of ffD; however, the inverse linear trend was not

Table 1 Characteristics of the study population

Variable	n (%) or mean (SD)		
	Cases (N = 249)	Controls (N = 368)	P-value
Sex (%)			
Male	93 (37.4)	141 (38.3)	0.81
Female	156 (62.7)	227 (61.7)	
Age (years)	68.5 (8.6)	66.6 (8.5)	0.006
Region of residence (%)			
Fukuoka	89 (35.7)	154 (41.9)	0.13
Kinki	160 (64.3)	214 (58.2)	
ffack-years of smoking (%)			
None	185 (74.3)	222 (60.3)	0.0004
0.1–29.9	37 (14.9)	65 (17.7)	
≥30.0	27 (10.8)	81 (22.0)	
Education (%)			
< 10 years	51 (20.5)	77 (20.9)	0.81
10–12 years	122 (49.0)	171 (46.5)	
≥13 years	76 (30.5)	120 (32.6)	
Body mass index (kg/m^2)	22.3 (3.3)	23.0 (3.4)	0.01
Daily intake[a]			
Total energy (kJ)	8435.4 (2636.8)	8348.8 (3067.5)	0.71
Total vegetables (g)	270.6 (149.4)	276.1 (181.9)	0.68
Green and yellow vegetables (g)	102.2 (64.8)	106.0 (84.8)	0.53
ff ther vegetables (g)	168.4 (110.6)	170.1 (132.3)	0.86
Total fruit (g)	180.7 (136.5)	166.5 (141.9)	0.22
Vitamin C (mg)	127.1 (64.2)	119.3 (70.2)	0.16
Vitamin E (mg)	8.6 (2.4)	8.4 (2.9)	0.52
α-Carotene (μg)	327.2 (314.1)	335.2 (339.2)	0.77
β-Carotene (μg)	3021.7 (1630.9)	3126.0 (2024.7)	0.48
Cryptoxanthin (μg)	454.8 (512.7)	329.4 (388.5)	0.001
Cholesterol (mg)	331.3 (129.5)	300.9 (132.5)	0.005
Alcohol (g)	5.5 (15.5)	10.0 (25.8)	0.008
Total dairy products (g)	132.2 (105.6)	137.6 (128.0)	0.57
Coffee (g)	119.0 (138.8)	172.7 (207.7)	0.0001
Dietary glycemic index	65.1 (4.7)	65.4 (5.3)	0.39

[a]Nutrient intake was adjusted for total energy intake using the residual method, except for the dietary glycemic index.

Table 2 ffdds ratios (ffRs) and 95% confidence intervals (CIs) for ffarkinson's disease by quartiles of intake of antioxidant vitamins

Variable	Quartile				*P* for trend
	1 (lowest)	2	3	4 (highest)	
Vitamin C					
Intake (mg/day)[a]	<84.7	84.7 to <109.6	109.6 to <147.7	≥147.7	
No. cases/controls	60/92	52/92	64/92	73/92	
Crude ffR (95% CI)	1.00	0.87 (0.54–1.39)	1.07 (0.68–1.68)	1.22 (0.78–1.91)	0.27
Multivariate ffR (95% CI)[b]	1.00	0.71 (0.43–1.19)	0.82 (0.49–1.37)	0.92 (0.54–1.55)	0.95
Vitamin E					
Intake (mg/day)[a]	<7.19	7.19 to <8.44	8.44 to <9.759	≥9.759	
No. cases/controls	73/92	55/92	54/92	67/92	
Crude ffR (95% CI)	1.00	0.75 (0.48–1.19)	0.74 (0.47–1.17)	0.92 (0.59–1.43)	0.68
Multivariate ffR (95% CI)[b]	1.00	0.49 (0.29–0.81)	0.41 (0.24–0.71)	0.45 (0.25–0.79)	0.009
α-Carotene					
Intake (μg/day)[a]	<137.5	137.5 to <262.6	262.6 to <504.3	≥504.3	
No. cases/controls	68/92	60/92	66/92	55/92	
Crude ffR (95% CI)	1.00	0.88 (0.56–1.39)	0.97 (0.62–1.52)	0.81 (0.51–1.28)	0.47
Multivariate ffR (95% CI)[b]	1.00	0.71 (0.43–1.15)	0.69 (0.42–1.13)	0.61 (0.36–1.02)	0.08
β-Carotene					
Intake (μg/day)[a]	<1836.1	1836.1 to <2906.4	2906.4 to <4080.9	≥4080.9	
No. cases/controls	61/92	73/92	61/92	54/92	
Crude ffR (95% CI)	1.00	1.20 (0.77–1.87)	1.00 (0.63–1.58)	0.89 (0.55–1.41)	0.46
Multivariate ffR (95% CI)[b]	1.00	0.80 (0.48–1.31)	0.64 (0.38–1.08)	0.56 (0.33–0.97)	0.03
Cryptoxanthin					
Intake (μg/day)[a]	<115.0	115.0 to <242.0	242.0 to <429.0	≥429.0	
No. cases/controls	63/92	42/92	50/92	94/92	
Crude ffR (95% CI)	1.00	0.67 (0.41–1.08)	0.79 (0.50–1.27)	1.49 (0.97–2.30)	0.03
Multivariate ffR (95% CI)[b]	1.00	0.52 (0.30–0.87)	0.60 (0.35–1.003)	1.16 (0.71–1.89)	0.30

[a]Quartiles were based on intake adjusted for energy intake using the residual method; [b]Adjusted for sex, age, region of residence, pack-years of smoking, years of education, body mass index and dietary intake of cholesterol, alcohol, total dairy products, and coffee and the dietary glycemic index.

Table 3 ffdds ratios (ffRs) and 95% confidence intervals (CIs) for ffarkinson's disease by quartiles of intake of vegetables and fruit

Variable	Quartile				*P* for trend
	1 (lowest)	2	3	4 (highest)	
Total vegetables					
Intake (g/day)[a]	<175.5	175.5 to <246.6	246.6 to <346.2	≥346.2	
No. cases/controls	62/92	70/92	61/92	56/92	
Crude ffR (95% CI)	1.00	1.13 (0.72–1.77)	0.98 (0.62–1.55)	0.90 (0.57–1.43)	0.55
Multivariate ffR (95% CI)[b]	1.00	0.81 (0.49–1.32)	0.70 (0.42–1.16)	0.69 (0.40–1.16)	0.14
Green and yellow vegetables					
Intake (g/day)[a]	<61.1	61.1 to <92.9	92.9 to <131.7	≥131.7	
No. cases/controls	71/92	58/92	54/92	66/92	
Crude ffR (95% CI)	1.00	0.82 (0.52–1.28)	0.76 (0.48–1.20)	0.93 (0.60–1.45)	0.68
Multivariate ffR (95% CI)[b]	1.00	0.64 (0.39–1.03)	0.56 (0.34–0.93)	0.66 (0.40–1.08)	0.10
ffther vegetables					
Intake (g/day)[a]	<101.1	101.1 to <148.05	148.05 to <210.9	≥210.9	
No. cases/controls	57/92	75/92	64/92	53/92	
Crude ffR (95% CI)	1.00	1.32 (0.84–2.07)	1.12 (0.71–1.78)	0.93 (0.58–1.49)	0.61
Multivariate ffR (95% CI)[b]	1.00	1.10 (0.68–1.79)	0.90 (0.54–1.49)	0.78 (0.46–1.33)	0.25
Total fruit					
Intake (g/day)[a]	<86.8	86.8 to <138.2	138.2 to <225.7	≥225.7	
No. cases/controls	56/92	56/92	69/92	68/92	
Crude ffR (95% CI)	1.00	1.00 (0.63–1.60)	1.23 (0.78–1.95)	1.21 (0.77–1.92)	0.28
Multivariate ffR (95% CI)[b]	1.00	0.94 (0.57–1.57)	0.98 (0.59–1.64)	0.97 (0.57–1.65)	0.96

[a]Quartiles were based on intake adjusted for energy intake using the residual method; [b]Adjusted for sex, age, region of residence, pack-years of smoking, years of education, body mass index and dietary intake of cholesterol, alcohol, total dairy products, and coffee and the dietary glycemic index.

Variable	Adjusted ffR (95% CI)[a]				P for trend
	Quartile 1	Quartile 2	Quartile 3	Quartile 4	
Vitamin E					
Men	1.00	0.53 (0.24–1.12)	0.75 (0.30–1.84)	0.56 (0.21–1.48)	0.30
Women	1.00	0.41 (0.19–0.84)	0.27 (0.13–0.55)	0.33 (0.15–0.71)	0.006
β-Carotene					
Men	1.00	1.03 (0.48–2.18)	1.14 (0.52–2.48)	1.17 (0.45–3.05)	0.69
Women	1.00	0.54 (0.27–1.08)	0.35 (0.16–0.73)	0.32 (0.15–0.64)	0.001

[a]Adjusted for age, region of residence, pack-years of smoking, years of education, body mass index and dietary intake of cholesterol, alcohol, total dairy products, and coffee and the dietary glycemic index.

Table 4 ffdds ratios (ffRs) and 95% confidence intervals (CIs) for ffarkinson's disease by quartiles of intake of vitamin E and β-carotene in men and women

significant in the multivariate model (Table 3). There were no evident associations between intake of total vegetables, vegetables other than green and yellow vegetables, or total fruit and ffD.

When subjects were stratified by sex, significant inverse relationships with intake of vitamin E and β-carotene were found only in women (Table 4). A significant interaction was observed in the association of intake of β-carotene, but not vitamin E, with ffD between men and women (P = 0.49 and 0.047 for homogeneity of ffR for intake of vitamin E and β-carotene in the highest quartile, respectively).

Discussion

The Singapore Chinese Health Study, a cohort study, found a significant inverse exposure–response relationship between vitamin E intake and the risk of ffD whereas intake of vitamin C and total carotenoids was not related to ffD [4]. In a pooled analysis from the Health ffrofessionals Follow-up Study and the Nurses' Health Study, dietary vitamin E intake was significantly inversely associated with the risk of ffD, particularly in women, whereas neither intake of total vitamins C or E, dietary vitamin C, α-carotene, or β-carotene or use of vitamin C or vitamin E supplements was related to ffD [5]. A cross-sectional study in the Netherlands reported a significant inverse association between vitamin E intake and ffD; however, no relationships were shown between intake of vitamin C or β-carotene and ffD [6]. ffur results regarding vitamin E, vitamin C, and α-carotene, but not β-carotene, are in agreement with these findings. Also the current findings are consistent with those of seven case–control studies [7–11,13,15] and a cohort study [14] showing a null association between vitamin C intake and ffD and those of a case–control study showing a null relationship between α-carotene intake and ffD [10]. Additionally, our results agree with those of a cohort study [18] and two case–control studies [9,17] that found no associations between intake of vegetables or fruit and ffD. ffn the other hand, the present results are at variance with those of seven case–control studies that showed a null association between vitamin E intake and ffD [7–13], those of 4 case–control studies showing a null relationship between β-carotene intake and ffD [7,8,10,13], and those of a case–control study showing a significant inverse exposure–response relationship between raw vegetable intake and ffD [19]. These discrepancies may be explained by differences in the study population and design, dietary assessment methods used, definitions of ffD applied, and confounders considered.

Findings from laboratory studies are inconsistent. Vitamin E deficient mice were more susceptible to 1-methyl-4-phenyl-1,2,3,6-tetrahydropyridine (MffiTffi) toxicity than controls, in terms of lethality and dopamine metabolite deletion in the substantia nigra [30]. Treatment of mice with a daily oral administration of moderate amounts of vitamin E did not influence the depletion of dopamine levels in the striatum following a high dose of MffiTffi [31]. Neither α-tocopherol nor β-carotene in massive doses had any protective effect for dopaminergic nigrostriatal neurons in marmosets injected with low doses of MffiTffi[32]. MffiTffi-induced neurodegeneration was not worsened by genetic vitamin E deficiency, whereas oral administration of vitamin E resulted in the partial protection of striatal dopaminergic terminals against MffiTffi toxicity in a mouse model using α-tocopherol transfer protein knockout mice [33]. With the use of α-tocopherol transfer protein knockout mice, it was reported that the protective effect of γ-tocopherol was stronger than that of α-tocopherol against MffiTffi-induced damage of dopaminergic neurons [34]. Estimate of vitamin E intake in our DHQ is based on only that of α-tocopherol intake. The observed inverse relationship between vitamin E intake and ffD might be ascribed to γ-tocopherol intake, given the high degree of correlation between intake of α-tocopherol and γ-tocopherol.

With respect to our results associated with β-carotene, ffno and Yamada reported that vitamin A, β-carotene, and coenzyme Q10 dose-dependently inhibited alpha-synuclein fibril formation from fresh

alpha-synuclein and destabilized preformed alpha-synuclein fibrils *in vitro* [35].

Estrogens function as neuroprotectants against nigro-striatal dopamine neurodegeneration [36]. The observed significant inverse relationships between intake of vitamin E and β-carotene and ffD risk in women, but not in men, might be explained by an effect modification of estrogens.

The lack of an association between vitamin C intake and ffD might be attributable to the fact that vitamin C is water soluble and does not readily cross the blood–brain barrier [16]. Alternatively, the hypouricemic effect of vitamin C might have interfered with its beneficial effect as a potent antioxidant [37]. The Health ffrofessionals Follow-up Study found a clear inverse relationship between the dietary urate index and the risk of ffD whereas vitamin C intake was not associated with ffD; however, vitamin C intake became significantly inversely related to ffD after further adjustment for the dietary urate index [14].

This study had methodological strengths. Cases were identified using strict diagnostic criteria: the possibility of misclassification of ffD is negligible. The response rate among cases was high (84%). Extensive data on potential confounders were controlled for. After adjustment for only non-dietary confounders, inverse exposure–response associations between intake of vitamin E and β-carotene and ffD were not significant (P for trend = 0.37 and 0.15, respectively). In this study, dietary confounders were of particular importance.

There are several limitations. ffur DHQ could only approximate consumption. The consequence would introduce a bias toward the null. ffur DHQ was designed to assess dietary intake for 1 month prior to completing the questionnaire. The dopamine deficiency in patients with ffD might affect their food preferences in the preclinical stage [38]. Moreover, some of the non-motor symptoms such as constipation and hyposmia might precede the onset of overt motor signs [39,40]. Such symptoms might also affect food choices. Thus, pre-symptomatic and/or post-symptomatic ffD could influence dietary habits in some cases, which would lead to misclassification of their true long-term dietary exposure. However, in this study, there was no difference in total energy intake between cases and controls and intake of vitamin E and β-carotene was not correlated with disease severity among cases. The results of a sensitivity analysis confined to cases < 3 years from onset (n = 109) were similar to those in the overall analysis: the adjusted ffR in the highest quartile was 0.45 (95% CI: 0.21–0.97, P for trend = 0.04) for vitamin E and 0.59 (95% CI: 0.27–1.26, P for trend = 0.07) for β-carotene. However, we cannot rule out the possibility that the observed inverse associations are a consequence of ffD.

ffur control subjects were selected from 3 of the 11 collaborating hospitals at which cases were recruited. The results of a sensitivity analysis restricted to cases who were recruited from three hospitals associated with control recruitment (n = 153) were similar to those in the overall analysis: the adjusted ffR in the highest quartile was 0.58 (95% CI: 0.30–1.14, P for trend = 0.13) for vitamin E and 0.72 (95% CI: 0.38–1.35, P for trend = 0.17) for β-carotene.

The percentage of subjects using vitamin C and/or multivitamin supplements weekly or more often was not large. The results of a sensitivity analysis excluding these supplement users (cases = 221, controls = 327) were similar to those in the overall analysis: the adjusted ffR in the highest quartile was 0.48 (95% CI: 0.25–0.89, P for trend = 0.03) for vitamin E and 0.62 (95% CI: 0.35–1.11, P for trend = 0.06) for β-carotene.

This is the first study to show a significant protective relationship between β-carotene intake and the risk of ffD. Also this study provides further evidence for a preventive association between vitamin E intake and ffD. Antioxidant vitamins deserve further investigation as measures that would possibly protect against ffD.

Acknowledgements

This study was supported by Health and Labour Sciences Research Grants, Research on Intractable Diseases, Research Committee on Epidemiology of Intractable Diseases from the Ministry of Health, Labour, and Welfare, Japan.

References

1. Lin MT, Beal MF. Mitochondrial dysfunction and oxidative stress in neurodegenerative diseases. *Nature* 2006; **443:** 787–795.
2. Sayre LM, fferry G, Smith MA. ffxidative stress and neurotoxicity. *Chem Res Toxicol* 2008; **21:** 172–188.
3. Ricciarelli R, Argellati F, ffronzato MA, Domenicotti C. Vitamin E and neurodegenerative diseases. *Mol Aspects Med* 2007; **28:** 591–606.
4. Tan LC, Koh Wffi Yuan JM, *et al.* Differential effects of black versus green tea on risk of ffarkinson's disease in the Singapore Chinese Health Study. *Am J Epidemiol* 2008; **167:** 553–560.
5. Zhang SM, Hernán MA, Chen H, Spiegelman D, Willett WC, Ascherio A. Intakes of vitamins E and C, carotenoids, vitamin supplements, and ffD risk. *Neurology* 2002; **59:** 1161–1169.
6. de Rijk MC, Breteler MM, den Breeijen JH, *et al.* Dietary antioxidants and ffarkinson disease. The Rotterdam Study. *Arch Neurol* 1997; **54:** 762–765.
7. ffbwers KM, Smith-Weller T, Franklin GM, Longstreth WT Jr, Swanson ffD, Checkoway H. ffarkinson's disease

risks associated with dietary iron, manganese, and other nutrient intakes. *Neurology* 2003; **60:** 1761–1766.
8. Johnson CC, Gorell JM, Rybicki BA, Sanders K, ffeterson EL. Adult nutrient intake as a risk factor for ffarkinson's disease. *Int J Epidemiol* 1999; **28:** 1102–1109.
9. Anderson C, Checkoway H, Franklin GM, Beresford S, Smith-Weller T, Swanson ffD. Dietary factors in ffarkinson's disease: the role of food groups and specific foods. *Mov Disord* 1999; **14:** 21–27.
10. Scheider WL, Hershey LA, Vena JE, Holmlund T, Marshall JR, Freudenheim JL. Dietary antioxidants and other dietary factors in the etiology of ffarkinson's disease. *Mov Disord* 1997; **12:** 190–196.
11. Logroscino G, Marder K, Cote L, Tang MX, Shea S, Mayeux R. Dietary lipids and antioxidants in ffarkinson's disease: a population-based, case–control study. *Ann Neurol* 1996; **39:** 89–94.
12. Morens DM, Grandinetti A, Waslien CI, ffark CB, Ross GW, White LR. Case–control study of idiopathic ffarkinson's disease and dietary vitamin E intake. *Neurology* 1996; **46:** 1270–1274.
13. Hellenbrand W, Boeing H, Robra Bffi *et al.* Diet and ffarkinson's disease. II: a possible role for the past intake of specific nutrients. Results from a self-administered food-frequency questionnaire in a case–control study. *Neurology* 1996; **47:** 644–650.
14. Gao X, Chen H, Choi HK, Curhan G, Schwarzschild MA, Ascherio A. Diet, urate, and ffarkinson's disease risk in men. *Am J Epidemiol* 2008; **167:** 831–838.
15. ffaganini-Hill A. Risk factors for parkinson's disease: the leisure world cohort study. *Neuroepidemiology* 2001; **20:** 118–124.
16. Etminan M, Gill SS, Samii A. Intake of vitamin E, vitamin C, and carotenoids and the risk of ffarkinson's disease: a meta-analysis. *Lancet Neurol* 2005; **4:** 362–365.
17. Ma L, Zhang L, Gao XH, *et al.* Dietary factors and smoking as risk factors for ffD in a rural population in China: a nested case–control study. *Acta Neurol Scand* 2006; **113:** 278–281.
18. Chen H, Zhang SM, Hernán MA, Willett WC, Ascherio A. Diet and ffarkinson's disease: a potential role of dairy products in men. *Ann Neurol* 2002; **52:** 793–801.
19. Hellenbrand W, Seidler A, Boeing H, *et al.* Diet and ffarkinson's disease. I: a possible role for the past intake of specific foods and food groups. Results from a self-administered food-frequency questionnaire in a case–control study. *Neurology* 1996; **47:** 636–643.
20. Hughes AJ, Daniel SE, Kilford L, Lees AJ. Accuracy of clinical diagnosis of idiopathic ffarkinson's disease: a clinico-pathological study of 100 cases. *J Neurol Neurosurg Psychiatry* 1992; **55:** 181–184.
21. Sasaki S, Yanagibori R, Amano K. Self-administered diet history questionnaire developed for health education: a relative validation of the test-version by comparison with 3-day diet record in women. *J Epidemiol* 1998; **8:** 203–215.
22. Sasaki S, Ushio F, Amano K, *et al.* Serum biomarker-based validation of a self-administered diet history questionnaire for Japanese subjects. *J Nutr Sci Vitaminol* 2000; **46:** 285–296.
23. Murakami K, Sasaki S, Takahashi Y, *et al.* Reproducibility and relative validity of dietary glycaemic index and load assessed with a self-administered diet-history questionnaire in Japanese adults. *Br J Nutr* 2008; **99:** 639–648.
24. Science and Technology Agency. *Standard Tables of Food Composition in Japan.* 5th revised and enlarged edn. Tokyo, Japan: ffrinting Bureau of the Ministry of Finance, 2005 (in Japanese).
25. Science and Technology Agency. *Standard Tables of Food Composition in Japan, Fatty Acids Section.* 5th revised and enlarged edn. Tokyo, Japan: ffrinting Bureau of the Ministry of Finance, 2005 (in Japanese).
26. Willett W, Stampfer MJ. Total energy intake: implications for epidemiologic analyses. *Am J Epidemiol* 1986; **124:** 17–27.
27. Tanaka K, Miyake Y, Fukushima W, *et al.* Active and passive smoking and risk of ffarkinson's disease. *Acta Neurol Scand* 2010; doi: 10.1111/j.1600-0404.2010.01327.x. [Epub ahead of print].
28. Miyake Y, Sasaki S, Tanaka K, *et al.* Dietary fat intake and risk of ffarkinson's disease: a case–control study in Japan. *J Neurol Sci* 2010; **288:** 117–122.
29. Murakami K, Miyake Y, Sasaki S, *et al.* Dietary glycemic index is inversely associated with the risk of ffarkinson's disease: a case–control study in Japan. *Nutrition* 2010; **26:** 515–521.
30. ffdunze IN, Klaidman LK, Adams JD Jr. MfffTffi toxicity in the mouse brain and vitamin E. *Neurosci Lett* 1990; **108:** 346–349.
31. Gong L, Daigneault EA, Acuff RV, Kostrzewa RM. Vitamin E supplements fail to protect mice from acute MfffTffi neurotoxicity. *Neuroreport* 1991; **2:** 544–546.
32. fferry TL, Yong VW, Hansen S, *et al.* α-Tocopherol and β-carotene do not protect marmosets against the dopaminergic neurotoxicity of N-methyl-4-phenyl-1,2,3,6-tetrahydropyridine. *J Neurol Sci* 1987; **81:** 321–331.
33. Ren YR, Nishida Y, Yoshimi K, *et al.* Genetic vitamin E deficiency does not affect MfffTffi susceptibility in the mouse brain. *J Neurochem* 2006; **98:** 1810–1816.
34. Itoh N, Masuo Y, Yoshida Y, Cynshi ff, Jishage K, Niki E. γ-Tocopherol attenuates MfffTffi-induced dopamine loss more efficiently than α-tocopherol in mouse brain. *Neurosci Lett* 2006; **403:** 136–140.
35. ffno K, Yamada M. Vitamin A potently destabilizes preformed alpha-synuclein fibrils *in vitro*: implications for Lewy body diseases. *Neurobiol Dis* 2007; **25:** 446–454.
36. Bourque M, Dluzen DE, Di ffaolo T. Neuroprotective actions of sex steroids in ffarkinson's disease. *Front Neuroendocrinol* 2009; **30:** 142–157.
37. Huang HY, Appel LJ, Choi MJ, *et al.* The effects of vitamin C supplementation on serum concentrations of uric acid: results of a randomized controlled trial. *Arthritis Rheum* 2005; **52:** 1843–1847.
38. Wang GJ, Volkow ND, Fowler JS. The role of dopamine in motivation for food in humans: implications for obesity. *Expert Opin Ther Targets* 2002; **6:** 601–609.
39. Abbott RD, ffetrovitch H, White LR, *et al.* Frequency of bowel movements and the future risk of ffarkinson's disease. *Neurology* 2001; **57:** 456–462.
40. ffonsen MM, Stoffers D, Booij J, van Eck-Smit BL, Wolters ECh, Berendse HW. Idiopathic hyposmia as a preclinical sign of ffarkinson's disease. *Ann Neurol* 2004; **56:** 173–181.

Appendix

ffther members of the Fukuoka Kinki ffarkinson's Disease Study Group are as follows: Yasuhiko Baba and Tomonori Kobayashi (Department of Neurology, Faculty of Medicine, Fukuoka University); Hideyuki Sawada, Eiji Mizuta, and Nagako Murase (Clinical Research Institute and Department of Neurology, Utano National Hospital); Tsuyoshi Tsutada and Hiroyuki Shimada (Department of Geriatrics and Neurology, ffsaka City University Graduate School of Medicine); Jun-ichi Kira (Department of Neurology, Neurological Institute, Graduate School of Medical Sciences, Kyushu University); Tameko Kihira and Tomoyoshi Kondo (Department of Neurology, Wakayama Medical University); Hidekazu Tomimoto (Department of Neurology, Kyoto University Graduate School of Medicine); Takayuki Taniwaki (Division of Respirology, Neurology, and Rheumatology, Department of Medicine, Kurume University School of Medicine); Hiroshi Sugiyama and Sonoyo Yoshida (Department of Neurology, Minami-Kyoto National Hospital); Harutoshi Fujimura and Tomoko Saito (Department of Neurology, Toneyama National Hospital); Kyoko Saida and Junko Fujitake (Department of Neurology, Kyoto City Hospital); Naoki Fujii (Department of Neurology, Neuro-Muscular Center, National ffmuta Hospital); Masatoshi Naito and Jun Arimizu (Department of ffrthopaedic Surgery, Faculty of Medicine, Fukuoka University); Takashi Nakagawa, Hirofumi Harada, and Takayuki Sueta (Department of fftorhinolaryngology, Faculty of Medicine, Fukuoka University); Toshihiro Kikuta and George Umemoto (Department of ffral and Maxillofacial Surgery, Faculty of Medicine, Fukuoka University); Eiichi Uchio and Hironori Migita (Department of ffphthalmology, Faculty of Medicine, Fukuoka University); Kenichi Kazuki, Yoichi Ito, and Hiroyoshi Iwaki (Department of ffrthopaedic Surgery, ffsaka City University Graduate School of Medicine); Kunihiko Siraki and Shinsuke Ataka (Department of ffphthalmology and Visual Sciences, ffsaka City University Graduate School of Medicine); Hideo Yaname and Rie Tochino (Department of fftolaryngology and Head and Neck Surgery, ffsaka City University Graduate School of Medicine); Teruichi Harada (Department of fflastic and Reconstructive Surgery, ffsaka City University Graduate School of Medicine); Yasushi Iwashita, Motoyuki Shimizu, Kenji Seki, and Keiji Ando (Department of ffrthopedic Surgery, Utano National Hospital).

Glycobiology vol. 20 no. 1 pp. 99–106, 2010
doi:10.1093/glycob/cwp152
Advance Access publication on September 23, 2009

Protective effect of *N*-glycan bisecting GlcNAc residues on β-amyloid production in Alzheimer's disease

Keiko Akasaka-Manya[2], Hiroshi Manya[2], Yoko Sakurai[2], Boguslaw S Wojczyk[3], Yasunori Kozutsumi[4], Yuko Saito[5], Naoyuki Taniguchi[6], Shigeo Murayama[5], Steven L Spitalnik[3], and Tamao Endo[1,2]

[2]Department of Glycobiology, Tokyo Metropolitan Institute of Gerontology, Foundation for Research on Aging and Promotion of Human Welfare, Itabashi-ku, Tokyo 173-0015, Japan; [3]Department of Pathology and Cell Biology, Columbia University Medical Center, New York, NY 10032, USA; [4]Laboratory of Membrane Biochemistry and Biophysics, Graduate School of Biostudies, Kyoto University, Sakyo-ku, Kyoto, 606-8501; [5]Department of Neuropathology, Tokyo Metropolitan Institute of Gerontology, Foundation for Research on Aging and Promotion of Human Welfare, Itabashi-ku, Tokyo 173-0015; and [6]Department of Disease Glycomics, The Institute of Scientific and Industrial Research, Osaka University, Ibaraki, Osaka 565-0047, Japan

Received on August 4, 2009; revised on September 14, 2009; accepted on September 15, 2009

Alteration of glycoprotein glycans often changes various properties of the target glycoprotein and contributes to a wide variety of diseases. Here, we focused on the *N*-glycans of amyloid precursor protein whose cleaved fragment, β-amyloid, is thought to cause much of the pathology of Alzheimer's disease (AD). We previously determined the *N*-glycan structures of normal and mutant amyloid precursor proteins (the Swedish type and the London type). In comparison with normal amyloid precursor protein, mutant amyloid precursor proteins had higher contents of bisecting GlcNAc residues. Because *N*-acetylglucosaminyltransferase III (GnT-III) is the glycosyltransferase responsible for synthesizing a bisecting GlcNAc residue, the current report measured GnT-III mRNA expression levels in the brains of AD patients. Interestingly, GnT-III mRNA expression was increased in AD brains. Furthermore, β-amyloid treatment increased GnT-III mRNA expression in Neuro2a mouse neuroblastoma cells. We then examined the influence of bisecting GlcNAc on the production of β-amyloid. Both β-amyloid 40 and β-amyloid 42 were significantly decreased in GnT-III-transfected cells. When secretase activities were analyzed in GnT-III transfectant cells, α-secretase activity was increased. Taken together, these results suggest that upregulation of GnT-III in AD brains may represent an adaptive response to protect them from additional β-amyloid production.

Keywords: Alzheimer's disease/amyloid precursor protein/bisecting GlcNAc/*N*-glycan

Introduction

Alzheimer's disease (AD) is a progressive neurodegenerative disorder characterized by global cognitive decline involving memory, orientation, judgment, and reasoning. The presence of extracellular senile plaques is one of the classical characteristics of AD pathology. β-Amyloid (Aβ), the major component of senile plaques, is a cleaved fragment of a membrane-spanning glycoprotein, amyloid precursor protein (APP). APP requires cleavage by the β- and γ-secretases to release soluble Aβ. In contrast, α-secretase cleaves APP within the Aβ sequence and prevents the generation of Aβ. Indeed, α-secretase competes with β-secretase for APP processing in the trans-Golgi network (Skovronsky et al. 2000). According to the "amyloid cascade hypothesis," the abnormal accumulation of Aβ leads to neurodegenerative processes, finally resulting in neuronal death. Two types of Aβ are produced depending on the γ-secretase cleavage site: Aβ40 and Aβ42. Aβ42 is a minor form of Aβ but has a greater tendency to produce insoluble deposits and is a major component of senile plaques.

Glycoproteins glycans affect protein stability, conformation, cellular localization, and trafficking (Wang et al. 2005; Ohtsubo and Marth 2006). APP undergoes several posttranslational modifications including *N*- and *O*-linked glycosylation (Weidemann et al. 1989; Tomita et al. 1998; Sato et al. 1999). Core *N*-glycosylation and *N*-glycan processing modulate the synthesis and expression of APP (Pahlsson et al. 1992; Saito et al. 1995; Yazaki et al. 1996). In addition, sialylation of APP *N*-glycans enhanced secretion of its metabolites (Nakagawa et al. 2006). These studies suggest that *N*-glycosylation status may affect the APP metabolic pathway; however, much remains unknown.

We previously determined the *N*-glycan structures of normal and mutant APPs (i.e., the Swedish and London types) (Akasaka-Manya et al. 2008). The Swedish type mutation (Lys595/Met596 to Asn/Leu) increases Aβ42 secretion by 6- to 7-fold (Citron et al. 1992) and the London type mutation (Val642 to Phe) doubles the ratio of secreted Aβ42 to Aβ40 (Suzuki et al. 1994; Price et al. 1998; Sinha and Lieberburg 1999). When the *N*-glycan structures of these mutant APPs were analyzed, we found an increased content of bisecting GlcNAc residues. This prompted us to study the expression levels of β1,4-*N*-acetylglucosaminyltransferase III (GnT-III) in the brains of AD patients because GnT-III is the glycosyltransferase responsible for adding bisecting GlcNAc during *N*-glycan processing (Nishikawa et al. 1992) (Figure 1). The presence of bisecting GlcNAc on individual *N*-glycans prevents the subsequent actions of several glycosyltransferases, including α-mannosidase II, GnT-II, GnT-IV, and GnT-V (Narasimhan 1982; Schachter et al. 1983; Schachter 1986). Thus, attachment of bisecting GlcNAc can significantly alter the types *N*-glycan structures that

[1]To whom correspondence should be addressed: Tel: +81-3-3964-3241 ext. 3080; Fax: +81-3-3579-4776; e-mail: endo@tmig.or.jp

© The Author 2009. Published by Oxford University Press. All rights reserved. For permissions, please e-mail: journals.permissions@oxfordjournals.org

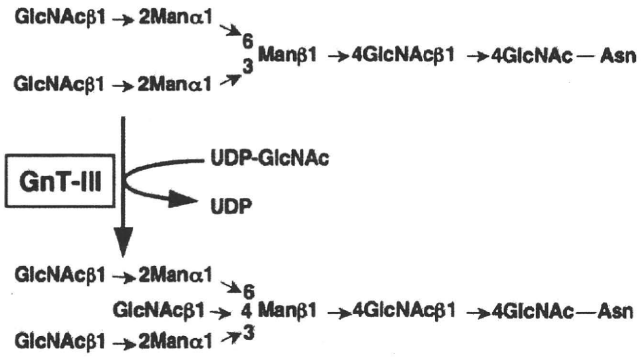

Fig. 1. Bisecting GlcNAc residues in *N*-glycans are synthesized by GnT-III.

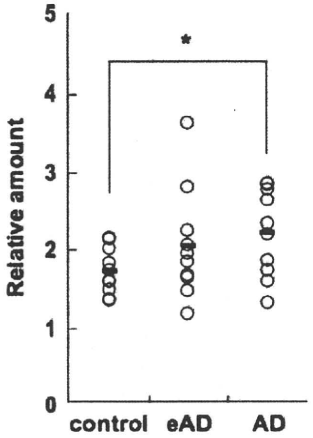

Fig. 2. Quantitative real-time RT-PCR analysis of *GnT-III* mRNA expression in brains of AD patients. Relative amounts of *GnT-III* mRNA were determined in 10 eAD patients, 10 AD patients, and 10 control subjects. All reactions were performed in triplicate and the open circles indicate average values for each individual brain sample. Each horizontal bar indicates the average value of the 10 subjects in that category. Statistically significant differences were identified using the Student's *t*-test ($P = 0.025$) and indicated with an asterisk.

are synthesized. Given the important biological functions of GnT-III (Gu and Taniguchi 2004), we examined the effects of the bisecting GlcNAc on Aβ production and on the activity of the various secretases responsible for Aβ production.

Results

GnT-III mRNA expression in the brains of AD patients

GnT-III catalyzes the transfer of GlcNAc to a core β-mannose residue, producing a bisecting GlcNAc (Wilson et al. 1976; Narasimhan 1982; Nishikawa et al. 1992). To investigate whether GnT-III levels are altered in AD, we measured the amount of *GnT-III* mRNA in the brains of AD patients by quantitative real-time RT-PCR. Preparation of total RNA from non-AD (control), early-stage AD (eAD), or AD brains and real-time RT-PCR analysis was performed as described in *Material and Methods*. As shown in Figure 2, the expression level of *GnT-III* mRNA was significantly increased in AD brains as compared to controls (mean relative amount of control, 1.74; standard deviation (SD), ± 0.28; mean relative amount of AD, 2.23; SD, ± 0.54; $P = 0.025$, Student's *t*-test). However, there was no statistically significant difference in *GnT-III* mRNA levels when comparing eAD brains to controls (mean relative amount of eAD, 2.06; SD, ± 0.68, $P = 0.21$, Student's *t*-test), or when comparing eAD brains to AD brains ($P = 0.56$, Student's *t*-test). Taken together, these results suggest that *GnT-III* mRNA expression increases with disease progression. Therefore, it is conceivable that the number of *N*-glycans having a bisecting GlcNAc residue is increased in AD brains.

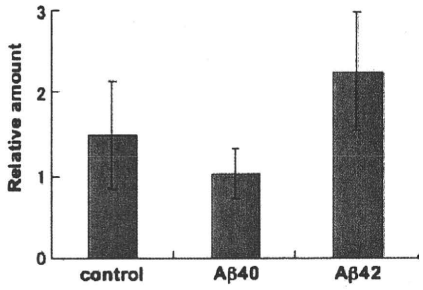

Fig. 3. Relative levels of *GnT-III* mRNA expression after incubation with Aβ. All reactions were performed in quadruplicate. Aβ40 or Aβ42 was added to Neuro2a cell culture medium at a final concentration of 2 μg/mL. After 48 h incubation, cells were harvested for RNA preparation followed by quantitative real-time RT-PCR. Average values ± 1 SD are shown.

Aβ42 exposure enhances GnT-III expression

We examined whether incubation with Aβ40 or Aβ42 affected *GnT-III* mRNA expression levels. Thus, after Aβ40 or Aβ42 was added to the culture media of Neuro2a cells, *GnT-III* expression level was analyzed by quantitative real-time RT-PCR (Figure 3). Compared to control cells (mean relative amount, 1.48; SD, ± 0.64), Aβ42 enhanced the *GnT-III* mRNA expression approximately 1.5-fold (mean relative amount, 2.24; SD, ± 0.72); in contrast, Aβ40 decreased the *GnT-III* expression (mean relative amount, 1.02; SD, ± 0.3). These results indicate that Aβ42, but not Aβ40, enhances GnT-III mRNA expression.

Effect of GnT-III on APP processing

According to our prior (Akasaka-Manya et al. 2008) and current (Figure 2) studies, it is likely that increased *GnT-III* mRNA levels increase the number of *N*-glycans having a bisecting GlcNAc residue. Therefore, we prepared stable transfectants of Neuro2a mouse neuroblastoma cells that express GnT-III by using an expression plasmid encoding *GnT-III*. The microsomal membrane fraction from the transfected cells was used as an enzyme source to measure GnT-III activity (Figure 4A). GnT-III activity was significantly increased in cells transfected with *GnT-III* (32.1 pmol/min/mg) as compared to cells transfected with the "empty" pCXN2 vector (mock transfectant, 0.1 pmol/min/mg). As expected, the intensity of staining by the *Phaseolus vulgaris* lectin E_4 (PHA-E_4), which specifically recognizes bisecting GlcNAc residues (Yamashita et al. 1983), was enhanced in cellular proteins prepared from *GnT-III*-transfected cells (Figure 4B), demonstrating that these proteins have a higher content of bisecting GlcNAc residues. There were no significant differences in the expression levels of membrane-bound APP and secreted APP (sAPP) (Figure 4C, upper-left panel and upper-right

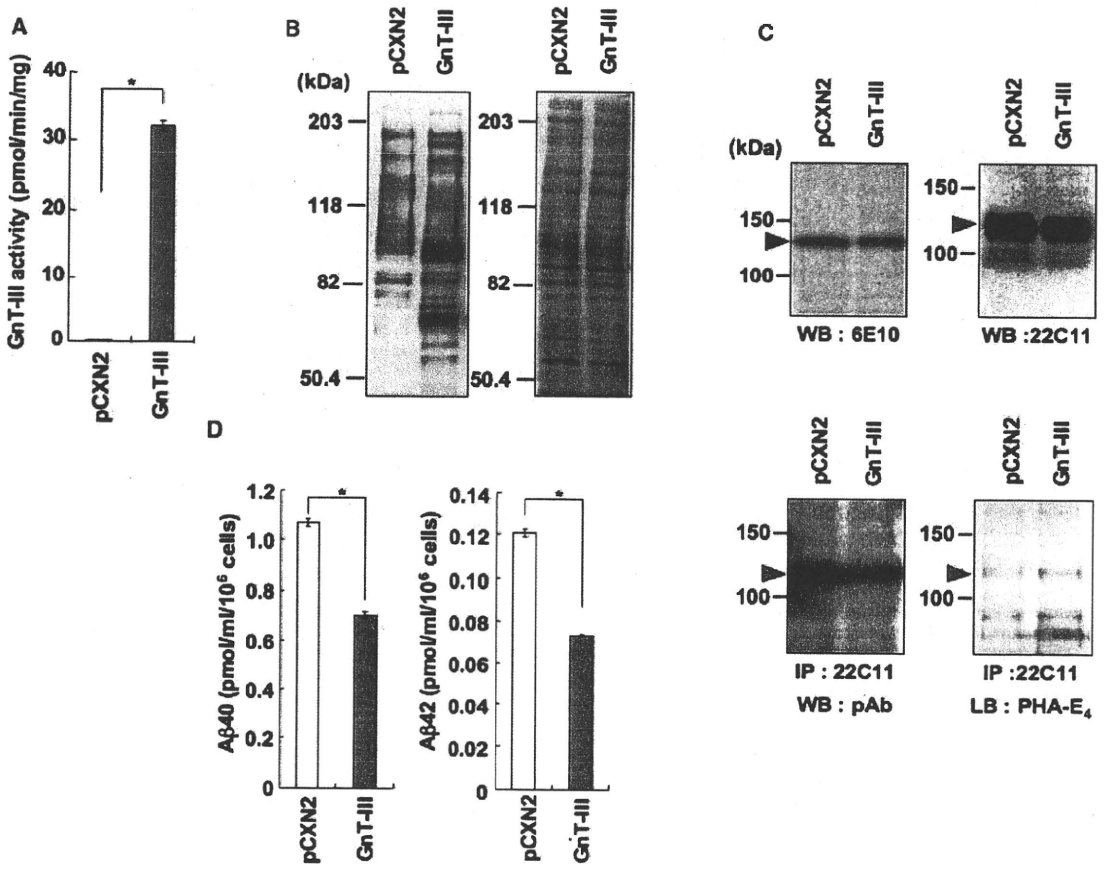

Fig. 4. Overexpression of *GnT-III* mRNA induces an increase in bisecting GlcNAc residues on cellular proteins and a decrease in Aβ secretion. (**A**) GnT-III activities of Neuro2a cells transfected with a *GnT-III* expression vector or an empty vector (pCXN2). Average values ± 1 SD of three independent experiments are shown. Asterisks indicate statistically significant differences ($P < 0.01$, Student's *t*-test). (**B**) Lectin (PHA-E_4) blot analysis of microsomal fraction of Neuro2a cells transfected with a *GnT-III* expression vector or an empty vector (pCXN2). Elevation of the bisecting GlcNAc modification was observed in *GnT-III*-transfected cells. Right panel indicates protein-staining patterns by Coomasie brilliant blue (CBB). Molecular weight standards are shown on the left. (**C**) Western blot analysis of membrane-bound APP or secreted APP (sAPP) in culture supernatants of Neuro2a cells transfected with a *GnT-III* expression vector or an empty vector (pCXN2). Membrane-bound APP was detected with an anti-APP monoclonal antibody (6E10) (upper-left panel) and sAPP in culture supernatant with an anti-APP monoclonal antibody (22C11) (upper-right panel). sAPP was immunoprecipitated from culture supernatant with an anti-APP monoclonal antibody (22C11), and then detected on blots by either an anti-APP polyclonal antibody (pAb, lower-left panel) or by the PHA-E_4 lectin (lower-right panel). Black triangle indicates membrane-bound APP and gray triangles indicate sAPP. Molecular weight standards are shown on the left. (**D**) The effect of GnT-III overexpression on Aβ production by transfected Neuro2a cells. Concentrations of Aβ40 (left) and Aβ42 (right) in culture supernatants were determined by ELISA. The average values ± 1 SD of three independent experiments are shown. Asterisks indicate statistically significant differences ($P < 0.01$, Student's *t*-test). pCXN2: stable mock transfectant of Neuro2a cells; GnT-III: stable transfectant of Neuro2a cells expressing GnT-III.

panel, respectively), but the intensity of PHA-E_4 staining of sAPP was enhanced in cells transfected with *GnT-III* (Figure 4C, lower-right panel). These results demonstrate that APP secreted from *GnT-III*-transfected cells has a higher content of bisecting GlcNAc residues.

We then measured levels of Aβ secreted by Neuro2a cells expressing recombinant GnT-III (Figure 4D). The concentrations of Aβ40 and Aβ42 secreted from the mock transfectant were 1.08 pmol/mL/10^6cells and 0.12 pmol/mL/10^6cells, respectively. For the *GnT-III* transfectant, the concentrations of Aβ40 and Aβ42 were 0.69 pmol/mL/10^6cells and 0.07 pmol/mL/10^6cells, respectively; these were 36.2% and 42.7% lower than those from the mock transfectant. These statistically significant results indicate that increased cellular expression of GnT-III significantly downregulates the secretion of Aβ peptides.

Western blot analysis of secretases

Contrary to our expectations, increased modification of *N*-glycans by bisecting GlcNAc downregulated Aβ secretion (Figure 4D). At least two mechanisms by which increased bisecting GlcNAc could reduce Aβ production should be considered. One possibility is that increasing bisecting GlcNAc expression on APP affects the conformation of APP, changing its susceptibility to α-, β-, and/or γ-secretase, and/or the intracellular localization of APP. Another possibility is that increasing the bisecting GlcNAc content of the secretases affects their enzymatic activity. α-Secretase activity is encoded by two proteins: ADAM 10 (a disintegrin and metalloproteinase 10) and tumor necrosis factor-α converting enzyme (TACE or, equivalently, ADAM 17). TACE has six potential *N*-glycosylation sites (Moss et al. 1997). ADAM 10 has four potential *N*-glycosylation sites, and their *N*-glycans are crucial for processing, localization, and

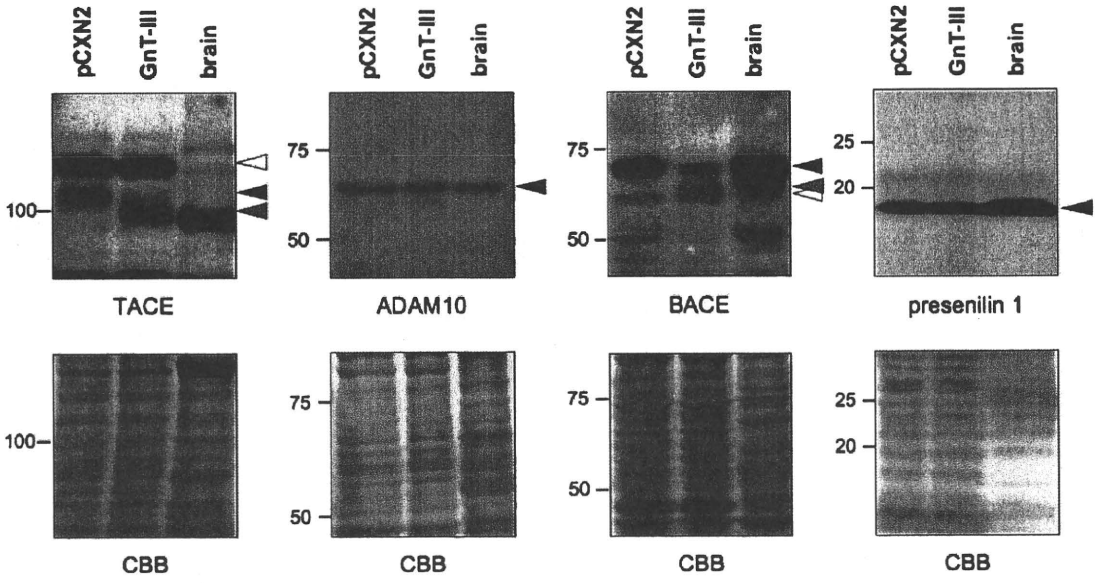

Fig. 5. Western blot analysis of various secretases (TACE, ADAM10, BACE, and presenilin) in *GnT-III*-transfected Neuro2a cells. For TACE and BACE, black and gray triangles indicate mature forms and white triangles indicate immature forms. For ADAM10 and presenilin 1, black triangles indicate the migration positions of ADAM10 and the C-terminal fragment of presenilin 1, respectively. Molecular weight standards are shown on the left. pCXN2: stable mock transfectant of Neuro2a cells; GnT-III: stable transfectant of Neuro2a cells expressing recombinant GnT-III; brain: mouse brain membrane fraction. Bottom figures indicate protein-staining patterns by CBB corresponding to each upper panel.

activity (Escrevente et al. 2008). BACE (β-site APP cleaving enzyme), which possesses β-secretase activity, has four potential *N*-glycosylation sites, three of them appear to be glycosylated (Charlwood et al. 2001). γ-Secretase is a protein complex consisting of presenilin, nicastrin, APH-1, and PEN-2. Nicastrin has 16 potential *N*-glycosylation sites, although inhibition of complex *N*-glycan processing does not affect γ-secretase activity (Herreman et al. 2003).

To clarify the mechanism(s) responsible for downregulating Aβ secretion, the expression levels of the secretases were measured. TACE is reported to change from an immature to a mature form (Milla et al. 1999; Schlondorff et al. 2000; Peiretti et al. 2003). Our Western blot analysis of TACE expressed by Neuro2a cells showed two major bands (Figure 5, left lane); results with proteins isolated from normal mouse brain are shown for comparison. The upper band (white triangle) corresponds to immature TACE bearing high-mannose *N*-glycans; the lower band corresponds to mature TACE (black triangle). Although two TACE bands were also observed in *GnT-III*-transfected Neuro2a cells (Figure 5, right lane), the mobility of mature TACE (gray triangle) from *GnT-III*-transfected cells was faster than that from the mock transfectant. As reported previously, this type of finding is a unique feature seen by introducing bisecting GlcNAc into glycoprotein *N*-glycans (Shigeta et al. 2006). In addition, the expression level of TACE in *GnT-III*-transfected cells was nearly the same as compared with mock transfectant. BACE is also reported to change from an immature form to a mature form (Benjannet et al. 2001; Schmechel et al. 2004). Our Western blot analysis of Neuro2a cells showed two BACE bands (Figure 5, left lane). The upper band corresponds to mature BACE (black triangle) and the lower to immature BACE (white triangle). An additional new band of intermediate mobility appeared in the *GnT-III*-transfected cells (Figure 5, gray triangle in the right lane). Interestingly, in the *GnT-III* transfectant, the

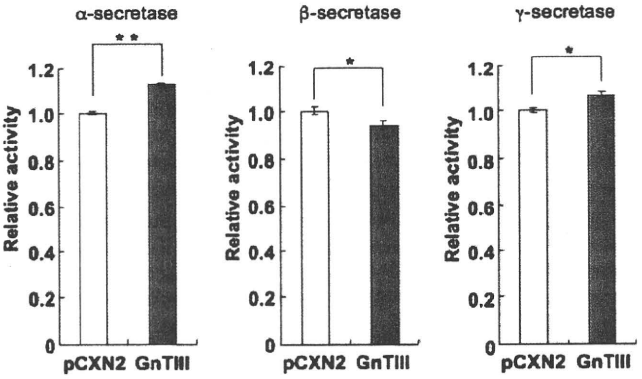

Fig. 6. Secretase activities in *GnT-III*-transfected Neuro2a cells. α-, β-, and γ-secretase activities (left, middle and right panels, respectively) were determined. For comparison, the fluorescence intensity of the pCXN2 transfectant was set to 1.0. The average percentages ± 1 SD of three independent experiments are shown. Asterisks indicate statistically significant differences ($^{*}P < 0.01$, $^{**}P = 0.0001$, Student's *t*-test).

molecular size and expression of BACE both decreased. In contrast, when comparing the mock transfectant with the *GnT-III* transfectant, no differences in the expression level or molecular size of ADAM 10 or the C-terminal fragment of presenilin 1 were seen (Thinakaran et al. 1996) (Figure 5). Taken together, these results suggest that changing the *N*-glycans of TACE and BACE may affect α- and β-secretase activities.

Secretase assays

To examine the effect of *N*-glycan changes of TACE and BACE on enzymatic activity, we measured α- and β-secretase activities in *GnT-III* transfectants of Neuro2a cells. As shown in Figure 6, in the *GnT-III* transfectant, α-secretase activity (113% of the

activity of the control pCXN2 transfectant, $P = 0.0001$) was slightly upregulated, but β-secretase activity (97% of the pCXN2 transfectant, $P = 0.042$) was modestly downregulated. Because changes in γ-secretase activity may also affect Aβ production, its activity in *GnT-III*-transfected cells was measured; modest upregulation was observed (107% of the pCXN2 transfectant, $P = 0.015$). Taken together, the increased α-secretase activity and decreased β-secretase activity in the *GnT-III* transfectant were the most probable cause of the reduction in Aβ production shown in Figure 4D. Thus, these results suggest that changes in *N*-glycan of TACE and BACE affect their enzymatic activities and lead to downregulation of Aβ production.

Discussion

In previous studies, we described the *N*-glycan structures of APP695 produced by Chinese hamster ovary cells (Sato et al. 1999) and the C17.2 mouse neural stem cell line (Akasaka-Manya et al. 2008). Recombinant APP695 in both cell lines had sialylated bi- and triantennary complex-type *N*-glycans with fucosylated and nonfucosylated trimannosyl cores. However, only APP695 produced by C17.2 cells had *N*-glycans containing bisecting GlcNAc. This may be due to cell-type-specific differences in *N*-glycan processing that can be found with various recombinant glycoproteins (Kagawa et al. 1988; Cumming 1991). To determine whether mutations in the *APP* gene alter the structures of processed *N*-glycans, we expressed two mutant recombinant APPs (i.e., the Swedish type and the London type) in transfected C17.2 cells. Structural analysis of these *N*-glycans revealed that the two mutant APPs had higher contents of bisecting GlcNAc and core-fucose residues as compared to wild-type APP. These results clearly showed that these slight changes in amino acid sequence affected *N*-glycan processing.

The glycosyltransferase responsible for adding the bisecting GlcNAc residue is GnT-III (Wilson et al. 1976; Narasimhan 1982; Nishikawa et al. 1992). To examine whether *GnT-III* mRNA levels are related to the pathogenesis of sporadic AD, we examined this issue by quantitative real-time RT-PCR using brains of normal individuals and AD patients. As shown in Figure 2, *GnT-III* mRNA levels were significantly increased in the brains of AD patients. This upregulation may affect AD pathogenesis because significant differences were found in patients with an advanced stage of AD. Interestingly, incubation of Neuro2a cells with Aβ42 increased *GnT-III* gene expression levels (Figure 3). In a recent report (Fiala et al. 2007), exposure of normal peripheral blood mononuclear cells to Aβ peptide upregulated transcription of *GnT-III* and led to increased Aβ clearance by phagocytosis; interestingly, mononuclear cells isolated from AD patients exhibited downregulated *GnT-III* gene expression and were defective in phagocytosis of Aβ. Since upregulation of GnT-III expression was associated with enhanced phagocytosis of Aβ, an increment of GnT-III levels in mononuclear cells may lead to improved Aβ clearance. In contrast, as reported here, increased expression of GnT-III in Neuro2a cells downregulated Aβ production (Figure 4D), and *GnT-III* mRNA levels were increased in AD brains (Figure 2). Taken together, these results suggest that upregulation of GnT-III in neuronal cells may diminish Aβ production in AD brains. In addition, expression of GnT-III in neurons and monocytes may modulate Aβ accumulation by different mechanisms. That is, upregulation of GnT-III expression in monocytes may enhance Aβ clearance, and increased GnT-III expression in neuronal cells may inhibit Aβ production. Taken together, both responses may be adaptive, protective responses that inhibit the further progression of AD.

To evaluate the mechanism by which an increased number of bisecting GlcNAc residues could reduce Aβ production, several possibilities should be considered. As reported here, the APP secreted by *GnT-III*-transfected Neuro2a cells has a higher content of bisecting GlcNAc than that secreted by control cells (Figure 4C). The addition of bisecting GlcNAc may affect the conformation of APP, thereby leading to a change in its susceptibility to α-, β-, and/or γ-secretases. Alteration of glycoprotein glycans is known to affect various properties of a given protein including its susceptibility to various modifying enzymes. For example, organ-specific differential glycosylation of low-density lipoprotein receptor-related protein 1 (LRP1) alters its proteolytic cleavage by γ-secretase (May et al. 2003). In addition, increased sialylation of APP enhanced Aβ secretion (Nakagawa et al. 2006). Bisecting GlcNAc residues are also known to affect the branching and elongation of various *N*-glycans antennae (Narasimhan 1982; Schachter et al. 1983; Schachter 1986). Therefore, it is possible that increasing bisecting GlcNAc expression on APP leads to changes in the APP *N*-glycan structure, including less sialylation, which may alter it susceptibility to cleavage by individual secretases (Fukuta et al. 2000; Koyota et al. 2001). Furthermore, because changing the *N*-glycan structure can alter intracellular glycoprotein localization, it is possible that bisecting GlcNAc affects APP trafficking and, thereby, its susceptibility to secretases. For example, in cells that overexpress GnT-III, cell surface turnover of E-cadherin is delayed (Yoshimura et al. 1996). In contrast, the cell surface expression of epidermal growth factor receptor is reduced in GnT-III overexpressing cells (Rebbaa et al. 1997). In addition, APP localization and trafficking vary according to its glycan modifications (McFarlane et al. 1999).

Another possibility is that increasing the bisecting GlcNAc content of the secretases affects their enzymatic activity. For example, glycosylation is known to play a critical role in maintaining the enzymatic activity of β-secretase (Charlwood et al. 2001). In that study, baculovirus-expressed β-secretase, which only has high-mannose-type *N*-glycans, exhibits only ~50% of the activity found when the enzyme is expressed by mammalian cells, when it has complex-type *N*-glycans (Charlwood et al. 2001). To investigate this issue, we measured secretase activities in *GnT-III*-transfected cells; α- and β-secretase activities were significantly increased and decreased, respectively (Figure 6). By Western blot analysis, the *N*-glycan structures of TACE and BACE are altered (Figure 5), perhaps explaining the changes in their enzymatic activities. In a previous study (Skovronsky et al. 2001), TACE-expressing neurons often colocalized with Aβ plaques. Our results showed that GnT-III expression was increased in AD brains (Figure 2) and that increases in GnT-III might decrease BACE expression (Figure 6). Taken together, it is likely that upregulation of GnT-III in AD brains induces changes in the APP processing enzymes, TACE and BACE, which may inhibit Aβ formation. Although the detailed mechanisms are not yet clear, this increased expression of GnT-III may homeostatically partially protect AD brains from further Aβ production.

Bisected *N*-glycans play important roles in neurological function in vitro and in vivo. For example, bisecting GlcNAc

regulated serum depletion-induced neuritogenesis (Shigeta et al. 2006). In addition, truncated, inactive GnT-III induced abnormal neurological phenotypes in mice (Bhattacharyya et al. 2002). As another example, changes in bisected *N*-glycans may be related to the pathogenesis of prion disease (Rudd et al. 1999). Therefore, further studies are required to understand the precise physiological and pathological roles of bisecting GlcNAc in brain development and function.

In summary, based on the current results, we propose that high expression of GnT-III in human AD brains reduces Aβ production and protects against further deterioration of neurological function during this disease process. Therefore, compounds that upregulate the expression of bisecting *N*-glycans may provide a novel therapeutic approach toward preventing or ameliorating AD.

Material and methods

Patients and controls

Human brain tissues were obtained from the Brain Bank for Aging Research (BBAR), which consists of consecutive autopsy cases from a general geriatric hospital with informed consent obtained from the relatives for each autopsy. The brains were handled using the BBAR protocol described previously (Fumimura et al. 2007). In brief, half of the brain was serially sections into 7 mm slices, snap-frozen using powdered dry ice, and stored at −80°C. To minimize RNA degradation, samples with the shortest postmortem intervals were selected for study. Two grams of frozen gray matter were sampled from the temporal pole of 10 cases each with AD, eAD, and age-matched normal controls. The diagnosis of AD was based on the BBAR criteria (Hughes et al. 1982; Murayama and Saito 2004), as follows: (1) clinical dementia rating (Hughes et al. 1982) ≥ 1; (2) Braak's senile plaque stage equal to C; and (3) the Braak's neurofibrillary tangle stage ≥ IV. The diagnosis of eAD was based on the following criteria: (1) clinical dementia rating, either 0 or 0.5; (2) Braak's senile plaque stage ≥ B; and (3) Braak's neurofibirillary tangle stage ≥ III. The criteria for designating brains as coming from normal controls included a clinical dementia rating of 0, Braak's senile plaque stage 0, and Braak's neurofibrillary tangle stage ≤ II. The age of the selected AD cases ranged from 79 to 98 years old (average of 88.2 years), and the postmortem interval from 1.8 to 17.7 h (average of 7.1 h). The age of the eAD cases ranged between 76 and 96 years (average of 90.3 years), and the postmortem interval between 1.2 and 39.9 h (average of 9.6 h). The age of the normal controls ranged from 68 to 86 years (average of 75.8 years), and the postmortem interval ranged from 1.5 to 29.1 h (average of 7.4 h). This study was approved by the Internal Review Board of Tokyo Metropolitan Institute of Gerontology and of Tokyo Metropolitan Geriatric Hospital.

Real-time RT-PCR analysis

Total RNA was isolated from a portion of each patient's brain using the guanidinium thiocyanate method with TRIzol (Invitrogen Corp., Carlsbad, CA), following the manufacturer's instructions. The integrity of the isolated total RNA was confirmed using an Agilent 2100 bioanalyzer (Agilent Technologies, Inc., Santa Clara, CA). Total RNA from Neuro2a cells was isolated using ISOGEN (Nippon Gene Co., Ltd, Tokyo, Japan), following the manufacturer's instructions. First-strand cDNAs were synthesized using 5 μg of total RNA, SuperScript II RNase H⁻ Reverse Transcriptase, and random primers (Invitrogen). The relative quantification of target mRNA was determined using a TaqMan real-time RT-PCR assay on a 7300 Fast Real-Time PCR System (Applied Biosystems, Foster City, CA), following the manufacturer's instructions using the TaqMan Universal PCR Master Mix and TaqMan Gene Expression Assays (i.e., a mixture of designed primers and TaqMan probes, Applied Biosystems): *GnT-III*, Hs02379589_s1; endogenous control, the TaqMan Ribosomal RNA Control Reagents VIC Probe. 18S rRNA was used as normalization control.

Cell culture and expression of GnT-III

Neuro2a mouse neuroblastoma cells were maintained in a mixture of Dulbecco's modified Eagle's medium and OptiMEM (1:1, v/v, Invitrogen) supplemented with 5% fetal bovine serum (Invitrogen), 2 mM L-glutamine, 100 units/mL penicillin, and 50 μg/mL streptomycin at 37°C in a 5% CO_2 atmosphere. The pCXN2-rat-*GnT-III* expression plasmid was described previously (Kitada et al. 2001). This plasmid was transfected into Neuro2a cells using Lipofectamine PLUS reagent (Invitrogen) according to the manufacturer's instructions. Stable transfectants were selected with G418 (Invitrogen) at 1 mg/mL. The culture supernatants of these transfectants were collected after 24 h incubation in Dulbecco's modified Eagle's medium:OptiMEM (1:1, v/v) supplemented with 0.2% fetal bovine serum. The cells were homogenized in 10 mM Tris-HCl, pH 7.4, 1 mM EDTA, 250 mM sucrose, 1 mM dithiothreitol, with protease inhibitor mixture (3 μg/mL pepstatin A, 1 μg/mL leupeptin, 1 mM benzamidine-HCl, 1 mM PMSF). After centrifugation at 900 × *g* for 10 min, the supernatant was centrifuged at 100,000 × *g* for 1 h; the pellet was used as the microsomal fraction. Protein concentration was determined by BCA assay (Thermo Fisher Scientific Inc., Waltham, MA).

Aβ treatment of Neuro2a cells was performed as follows: Aβ40 and Aβ42 were each purchased from PEPTIDE INSTITUTE, INC. (Osaka, Japan) and dissolved in H_2O. Aβ40 or Aβ42 were added to culture medium at a final concentration of 2 μg/mL. Cells were cultured for 48 h and harvested for RNA preparation followed by real-time RT-PCR.

Preparation of mouse brain membrane fraction

Brains were obtained from 4-week-old C57BL/6 mice, and homogenized with 9 volumes (weight/volume) of 10 mM Tris-HCl, pH 7.4, 1 mM EDTA, 250 mM sucrose. After centrifugation at 900 × *g* for 10 min, the supernatant was centrifuged at 100,000 × *g* for 1 h; the pellet was used as the microsomal membrane fraction. Protein concentration was determined by BCA assay. All experimental procedures using laboratory animals were approved by the Animal Care and Use Committee of Tokyo Metropolitan Institute of Gerontology.

Assay for GnT-III activity

GnT-III activity was measured using a modification of a previously reported method (Taniguchi et al. 1989). The enzyme assay mixture, containing 125 mM MES buffer (pH 6.25), 200 mM GlcNAc, 10 mM $MnCl_2$, 20 mM UDP-GlcNAc, 0.5% Triton X-100, 10 μM of 2-aminobenzamide-labeled [GlcNAcβ1-2Manα1-6 (GlcNAcβ1-2Manα1-3) Manβ1-4Glc

NAcβ1-4GlcNAc] (ProZyme, Leandro, CA), and cell homogenate were incubated at 37°C for 1 h. After boiling for 3 min to stop the reaction, the mixture was subjected to reversed-phase HPLC using a Cosmosil 5C18-AR column (Nacalai Tesque, Kyoto, Japan), which was equilibrated with the 100 mM ammonium acetate buffer, pH 4.0, and eluted with a gradient of 1-butanol (0.25–1% butanol) over 120 min at a flow rate of 1 mL/min at 55°C.

Immunoprecipitation

For APP immunoprecipitation, culture supernatants were mixed with an anti-APP monoclonal antibody (22C11, Millipore, Billerica, MA). After incubation at 4°C for 2 h, Protein G-coupled Sepharose-4B beads (GE Healthcare UK Ltd., Buckinghamshire, England) were added and the mixture rotated at 4°C for 2 h. The beads were washed three times with PBS and suspended in the sample buffer. Immunoprecipitated proteins were recovered by boiling for 3 min and then subjected to Western blot and lectin blot analyses.

Western blot analysis

Proteins were separated by SDS–PAGE (for TACE, a 5–10% gradient gel; for APP, BACE, and ADAM 10, a 7.5% gel; for presenilin 1, a 12.5% gel) and transferred to a PVDF membrane. The membrane, after blocking in PBS containing 5% skim milk and 0.05% Tween 20, was incubated with an anti-APP polyclonal antibody (Millipore, Billerica, MA) or an anti-APP monoclonal antibody (6E10, Signet laboratories, Dedham, MA). The membrane was then incubated with anti-rabbit IgG conjugated with horseradish peroxidase (GE Healthcare). Antibody-bound proteins were visualized using an ECL kit (GE Healthcare).

Secretases in the microsomal fractions were visualized after separation by SDS–PAGE using anti-TACE polyclonal antibody (Thermo Fisher Scientific), anti-ADAM10 antibody, anti-presenilin 1 antibody, and anti-BACE antibody (Abcam, Cambridge, England).

Lectin blot analysis

Immunoprecipitated proteins were separated by SDS–PAGE and transferred to a PVDF membrane. After blocking with 3% bovine serum albumin (BSA, Nacalai Tesque) in 10 mM Tris-HCl (pH 7.4) containing 140 mM NaCl, 1 mM $CaCl_2$, 1 mM $MgCl_2$, 1 mM $MnCl_2$, and 0.05% Tween 20 (TBS-T), the membrane was incubated with biotin-conjugated PHA-E_4 (Seikagaku Corporation, Tokyo, Japan) in TBS-T containing 1% BSA. After treating the membrane with the Vectastain ABC kit (Vector, Burlingame, CA), lectin-bound proteins were visualized with an ECL kit.

Quantification of soluble Aβ by sandwich ELISA

Culture supernatants were subjected to enzyme-linked immunosorbent assay (ELISA) using the Human/Rat β-Amyloid 40 ELISA kit II and the Human/Rat β-Amyloid 42 ELISA kit High Sensitive (Wako Pure Chemical Industries, Ltd., Osaka, Japan) according to manufacturer's instructions.

Secretase assays

Secretase enzymatic assays were performed using the α-secretase assay kit, β-secretase assay kit, and γ-secretase assay kit (R & D Systems, Inc., Minneapolis, MN), according to manufacturer's instructions. Briefly, cultured Neuro2a cells were harvested and cell numbers counted. Cells were lysed with the extraction buffer and used as an enzyme source for the assay. An APP peptide conjugated to fluorescent reporter and quencher was used as the substrate. The protein content of cell lysates was determined by BCA assay and secretase activities were normalized to protein concentration.

Funding

The Japan Society for the Promotion of Science (20390031).

Acknowledgements

We thank Ms. Harumi Yamamoto and Ms. Reiko Fujinawa for technical assistance.

Conflict of interest statement

None declared.

Abbreviations

Aβ, β-amyloid; AD, Alzheimer's disease; ADAM, a disintegrin and metalloprotease; APP, amyloid precursor protein; BACE, β-site APP-cleaving enzyme; eAD, early-stage AD; GnT, *N*-acetylglucosaminyltransferase; TACE, tumor necrosis factor-α-converting enzyme.

References

Akasaka-Manya K, Manya H, Sakurai Y, Wojczyk BS, Spitalnik SL, Endo T. 2008. Increased bisecting and core-fucosylated *N*-glycans on mutant human amyloid precursor proteins. *Glycoconj J.* 25:775–786.

Benjannet S, Elagoz A, Wickham L, Mamarbachi M, Munzer JS, Basak A, Lazure C, Cromlish JA, Sisodia S, Checler F, et al. 2001. Post-translational processing of β-secretase (β-amyloid-converting enzyme) and its ectodomain shedding. The pro- and transmembrane/cytosolic domains affect its cellular activity and amyloid-β production. *J Biol Chem.* 276:10879–10887.

Bhattacharyya R, Bhaumik M, Raju TS, Stanley P. 2002. Truncated, inactive *N*-acetylglucosaminyltransferase III (GlcNAc-TIII) induces neurological and other traits absent in mice that lack GlcNAc-TIII. *J Biol Chem.* 277:26300–26309.

Charlwood J, Dingwall C, Matico R, Hussain I, Johanson K, Moore S, Powell DJ, Skehel JM, Ratcliffe S, Clarke B, et al. 2001. Characterization of the glycosylation profiles of Alzheimer's β-secretase protein Asp-2 expressed in a variety of cell lines. *J Biol Chem.* 276:16739–16748.

Citron M, Oltersdorf T, Haass C, McConlogue L, Hung AY, Seubert P, Vigo-Pelfrey C, Lieberburg I, Selkoe DJ. 1992. Mutation of the β-amyloid precursor protein in familial Alzheimer's disease increases β-protein production. *Nature.* 360:672–674.

Cumming DA. 1991. Glycosylation of recombinant protein therapeutics: Control and functional implications. *Glycobiology.* 1:115–130.

Escrevente C, Morais VA, Keller S, Soares CM, Altevogt P, Costa J. 2008. Functional role of *N*-glycosylation from ADAM10 in processing, localization and activity of the enzyme. *Biochim Biophys Acta.* 1780:905–913.

Fiala M, Liu PT, Espinosa-Jeffrey A, Rosenthal MJ, Bernard G, Ringman JM, Sayre J, Zhang L, Zaghi J, Dejbakhsh S, et al. 2007. Innate immunity and transcription of MGAT-III and Toll-like receptors in Alzheimer's disease patients are improved by bisdemethoxycurcumin. *Proc Natl Acad Sci USA.* 104:12849–12854.

Fukuta K, Abe R, Yokomatsu T, Omae F, Asanagi M, Makino T. 2000. Control of bisecting GlcNAc addition to *N*-linked sugar chains. *J Biol Chem.* 275:23456–23461.

Fumimura Y, Ikemura M, Saito Y, Sengoku R, Kanemaru K, Sawabe M, Arai T, Ito G, Iwatsubo T, Fukayama M, et al. 2007. Analysis of the adrenal gland is useful for evaluating pathology of the peripheral autonomic nervous system in Lewy body disease. *J Neuropathol Exp Neurol.* 66:354–362.

Gu J, Taniguchi N. 2004. Regulation of integrin functions by *N*-glycans. *Glycoconj J.* 21:9–15.

Herreman A, Van Gassen G, Bentahir M, Nyabi O, Craessaerts K, Mueller U, Annaert W, De Strooper B. 2003. γ-Secretase activity requires the presenilin-dependent trafficking of nicastrin through the Golgi apparatus but not its complex glycosylation. *J Cell Sci.* 116:1127–1136.

Hughes CP, Berg L, Danziger WL, Coben LA, Martin RL. 1982. A new clinical scale for the staging of dementia. *Br J Psychiatry.* 140:566–572.

Kagawa Y, Takasaki S, Utsumi J, Hosoi K, Shimizu H, Kochibe N, Kobata A. 1988. Comparative study of the asparagine-linked sugar chains of natural human interferon-β 1 and recombinant human interferon-β 1 produced by three different mammalian cells. *J Biol Chem.* 263:17508–17515.

Kitada T, Miyoshi E, Noda K, Higashiyama S, Ihara H, Matsuura N, Hayashi N, Kawata S, Matsuzawa Y, Taniguchi N. 2001. The addition of bisecting *N*-acetylglucosamine residues to E-cadherin down-regulates the tyrosine phosphorylation of β-catenin. *J Biol Chem.* 276:475–480.

Koyota S, Ikeda Y, Miyagawa S, Ihara H, Koma M, Honke K, Shirakura R, Taniguchi N. 2001. Down-regulation of the α-Gal epitope expression in *N*-glycans of swine endothelial cells by transfection with the *N*-acetylglucosaminyltransferase III gene. Modulation of the biosynthesis of terminal structures by a bisecting GlcNAc. *J Biol Chem.* 276:32867–32874.

May P, Bock HH, Nimpf J, Herz J. 2003. Differential glycosylation regulates processing of lipoprotein receptors by γ-secretase. *J Biol Chem.* 278:37386–37392.

McFarlane I, Georgopoulou N, Coughlan CM, Gillian AM, Breen KC. 1999. The role of the protein glycosylation state in the control of cellular transport of the amyloid β precursor protein. *Neuroscience.* 90:15–25.

Milla ME, Leesnitzer MA, Moss ML, Clay WC, Carter HL, Miller AB, Su JL, Lambert MH, Willard DH, Sheeley DM, et al. 1999. Specific sequence elements are required for the expression of functional tumor necrosis factor-α-converting enzyme (TACE). *J Biol Chem.* 274:30563–30570.

Moss ML, Jin SL, Milla ME, Bickett DM, Burkhart W, Carter HL, Chen WJ, Clay WC, Didsbury JR, Hassler D, et al. 1997. Cloning of a disintegrin metalloproteinase that processes precursor tumour-necrosis factor-α. *Nature.* 385: 733–736.

Murayama S, Saito Y. 2004. Neuropathological diagnostic criteria for Alzheimer's disease. *Neuropathology.* 24:254–260.

Nakagawa K, Kitazume S, Oka R, Maruyama K, Saido TC, Sato Y, Endo T, Hashimoto Y. 2006. Sialylation enhances the secretion of neurotoxic amyloid-β peptides. *J Neurochem.* 96:924–933.

Narasimhan S. 1982. Control of glycoprotein synthesis. UDP-GlcNAc:glycopeptide β 4-*N*-acetylglucosaminyltransferase III, an enzyme in hen oviduct which adds GlcNAc in β 1–4 linkage to the beta-linked mannose of the trimannosyl core of *N*-glycosyl oligosaccharides. *J Biol Chem.* 257:10235–10242.

Nishikawa A, Ihara Y, Hatakeyama M, Kangawa K, Taniguchi N. 1992. Purification, cDNA cloning, and expression of UDP-*N*-acetylglucosamine: β-D-mannoside β-1,4*N*-acetylglucosaminyltransferase III from rat kidney. *J Biol Chem.* 267:18199–18204.

Ohtsubo K, Marth JD. 2006. Glycosylation in cellular mechanisms of health and disease. *Cell.* 126:855–867.

Pahlsson P, Shakin-Eshleman SH, Spitalnik SL. 1992. *N*-Linked glycosylation of β -amyloid precursor protein. *Biochem Biophys Res Commun.* 189:1667–1673.

Peiretti F, Canault M, Deprez-Beauclair P, Berthet V, Bonardo B, Juhan-Vague I, Nalbone G. 2003. Intracellular maturation and transport of tumor necrosis factor α converting enzyme. *Exp Cell Res.* 285:278–285.

Price DL, Sisodia SS, Borchelt DR. 1998. Genetic neurodegenerative diseases: The human illness and transgenic models. *Science.* 282:1079–1083.

Rebbaa A, Yamamoto H, Saito T, Meuillet E, Kim P, Kersey DS, Bremer EG, Taniguchi N, Moskal JR. 1997. Gene transfection-mediated overexpression of β 1,4-*N*-acetylglucosamine bisecting oligosaccharides in glioma cell line U373 MG inhibits epidermal growth factor receptor function. *J Biol Chem.* 272:9275–9279.

Rudd PM, Endo T, Colominas C, Groth D, Wheeler SF, Harvey DJ, Wormald MR, Serban H, Prusiner SB, Kobata A, et al. 1999. Glycosylation differences between the normal and pathogenic prion protein isoforms. *Proc Natl Acad Sci USA.* 96:13044–13049.

Saito F, Tani A, Miyatake T, Yanagisawa K. 1995. *N*-Linked oligosaccharide of β-amyloid precursor protein (β APP) of C6 glioma cells: Putative regulatory role in β APP processing. *Biochem Biophys Res Commun.* 210:703–710.

Sato Y, Liu C, Wojczyk BS, Kobata A, Spitalnik SL, Endo T. 1999. Study of the sugar chains of recombinant human amyloid precursor protein produced by Chinese hamster ovary cells. *Biochim Biophys Acta.* 1472:344–358.

Schachter H. 1986. Biosynthetic controls that determine the branching and microheterogeneity of protein-bound oligosaccharides. *Biochem Cell Biol.* 64:163–181.

Schachter H, Narasimhan S, Gleeson P, Vella G. 1983. Control of branching during the biosynthesis of asparagine-linked oligosaccharides. *Can J Biochem Cell Biol.* 61:1049–1066.

Schlondorff J, Becherer JD, Blobel CP. 2000. Intracellular maturation and localization of the tumour necrosis factor α convertase (TACE). *Biochem J.* 347(Pt 1):131–138.

Schmechel A, Strauss M, Schlicksupp A, Pipkorn R, Haass C, Bayer TA, Multhaup G. 2004. Human BACE forms dimers and colocalizes with APP. *J Biol Chem.* 279:39710–39717.

Shigeta M, Shibukawa Y, Ihara H, Miyoshi E, Taniguchi N, Gu J. 2006. β 1,4-*N*-acetylglucosaminyltransferase III potentiates β1 integrin-mediated neuritogenesis induced by serum deprivation in Neuro2a cells. *Glycobiology.* 16:564–571.

Sinha S, Lieberburg I. 1999. Cellular mechanisms of β-amyloid production and secretion. *Proc Natl Acad Sci USA.* 96:11049–11053.

Skovronsky DM, Fath S, Lee VM, Milla ME. 2001. Neuronal localization of the TNFα converting enzyme (TACE) in brain tissue and its correlation to amyloid plaques. *J Neurobiol.* 49:40–46.

Skovronsky DM, Moore DB, Milla ME, Doms RW, Lee VM. 2000. Protein kinase C-dependent α-secretase competes with β-secretase for cleavage of amyloid-β precursor protein in the trans-Golgi network. *J Biol Chem.* 275:2568–2575.

Suzuki N, Cheung TT, Cai XD, Odaka A, Otvos L Jr, Eckman C, Golde TE, Younkin SG. 1994. An increased percentage of long amyloid β protein secreted by familial amyloid β protein precursor (β APP717) mutants. *Science.* 264:1336–1340.

Taniguchi N, Nishikawa A, Fujii S, Gu JG. 1989. Glycosyltransferase assays using pyridylaminated acceptors: *N*-acetylglucosaminyltransferase III, IV, and V. *Methods Enzymol.* 179:397–408.

Thinakaran G, Borchelt DR, Lee MK, Slunt HH, Spitzer L, Kim G, Ratovitsky T, Davenport F, Nordstedt C, Seeger M, et al. 1996. Endoproteolysis of presenilin 1 and accumulation of processed derivatives in vivo. *Neuron.* 17:181–190.

Tomita S, Kirino Y, Suzuki T. 1998. Cleavage of Alzheimer's amyloid precursor protein (APP) by secretases occurs after *O*-glycosylation of APP in the protein secretory pathway. Identification of intracellular compartments in which APP cleavage occurs without using toxic agents that interfere with protein metabolism. *J Biol Chem.* 273:6277–6284.

Wang X, Inoue S, Gu J, Miyoshi E, Noda K, Li W, Mizuno-Horikawa Y, Nakano M, Asahi M, Takahashi M, et al. 2005. Dysregulation of TGF-β1 receptor activation leads to abnormal lung development and emphysema-like phenotype in core fucose-deficient mice. *Proc Natl Acad Sci USA.* 102:15791–15796.

Weidemann A, Konig G, Bunke D, Fischer P, Salbaum JM, Masters CL, Beyreuther K. 1989. Identification, biogenesis, and localization of precursors of Alzheimer's disease A4 amyloid protein. *Cell.* 57:115–126.

Wilson JR, Williams D, Schachter H. 1976. The control of glycoprotein synthesis: *N*-acetylglucosamine linkage to a mannose residue as a signal for the attachment of L-fucose to the asparagine-linked *N*-acetylglucosamine residue of glycopeptide from α1-acid glycoprotein. *Biochem Biophys Res Commun.* 72:909–916.

Yamashita K, Hitoi A, Kobata A. 1983. Structural determinants of Phaseolus vulgaris erythroagglutinating lectin for oligosaccharides. *J Biol Chem.* 258:14753–14755.

Yazaki M, Tagawa K, Maruyama K, Sorimachi H, Tsuchiya T, Ishiura S, Suzuki K. 1996. Mutation of potential *N*-linked glycosylation sites in the Alzheimer's disease amyloid precursor protein (APP). *Neurosci Lett.* 221:57–60.

Yoshimura M, Ihara Y, Matsuzawa Y, Taniguchi N. 1996. Aberrant glycosylation of E-cadherin enhances cell-cell binding to suppress metastasis. *J Biol Chem.* 271:13811–13815.

Eur J Nucl Med Mol Imaging
DOI 10.1007/s00259-009-1202-1

ORIGINAL ARTICLE

Validation of cardiac ^{123}I-MIBG scintigraphy in patients with Parkinson's disease who were diagnosed with dopamine PET

Kenji Ishibashi · Yuko Saito · Shigeo Murayama · Kazutomi Kanemaru · Keiichi Oda · Kiichi Ishiwata · Hidehiro Mizusawa · Kenji Ishii

Received: 11 March 2009 / Accepted: 9 June 2009
© Springer-Verlag 2009

Abstract
Purpose The aim of this study was to evaluate the diagnostic potential of cardiac ^{123}I-labelled metaiodobenzylguanidine (^{123}I-MIBG) scintigraphy in idiopathic Parkinson's disease (PD). The diagnosis was confirmed by positron emission tomography (PET) imaging with ^{11}C-labelled 2β-carbomethoxy-3β-(4-fluorophenyl)-tropane (^{11}C-CFT) and ^{11}C-raclopride (together designated as dopamine PET).
Methods Cardiac ^{123}I-MIBG scintigraphy and dopamine PET were performed for 39 parkinsonian patients. To estimate the cardiac ^{123}I-MIBG uptake, heart to mediastinum (H/M) ratios in early and delayed images were calculated. On the basis of established clinical criteria and our dopamine PET findings, 24 patients were classified into the PD group and 15 into the non-PD (NPD) group.
Results Both early and delayed images showed that the H/M ratios were significantly lower in the PD group than in the NPD group. When the optimal cut-off levels of the H/M ratio were set at 1.95 and 1.60 in the early and delayed images, respectively, by receiver-operating characteristic analysis, the sensitivity of cardiac ^{123}I-MIBG scintigraphy for the diagnosis of PD was 79.2 and 70.8% and the specificity was 93.3 and 93.3% in the early and delayed images, respectively. In the Hoehn and Yahr 1 and 2 PD patients, the sensitivity decreased by 69.2 and 53.8% in the early and delayed images, respectively.
Conclusion In early PD cases, cardiac ^{123}I-MIBG scintigraphy is of limited value in the diagnosis, because of its relatively lower sensitivity. However, because of its high specificity for the overall cases, cardiac ^{123}I-MIBG scintigraphy may assist in the diagnosis of PD in a complementary role with the dopaminergic neuroimaging.

Keywords ^{123}I-MIBG · ^{11}C-CFT · ^{11}C-Raclopride · Scintigraphy · Positron emission tomography · Parkinson's disease

An Editorial Commentary on this paper is available at http://dx.doi.org/10.1007/s00259-009-1215-9.

K. Ishibashi · H. Mizusawa
Department of Neurology and Neurological Science,
Graduate School, Tokyo Medical and Dental University,
Tokyo, Japan

K. Ishibashi · K. Oda · K. Ishiwata · K. Ishii (✉)
Positron Medical Center,
Tokyo Metropolitan Institute of Gerontology,
1-1 Nakacho, Itabashi-ku,
Tokyo 173-0022, Japan
e-mail: ishii@pet.tmig.or.jp

Y. Saito
Department of Pathology, Tokyo Metropolitan Geriatric Hospital,
Tokyo, Japan

Y. Saito · S. Murayama
Department of Neuropathology,
Tokyo Metropolitan Institute of Gerontology,
Tokyo, Japan

K. Kanemaru
Department of Neurology, Tokyo Metropolitan Geriatric Hospital,
Tokyo, Japan

Published online: 22 July 2009

Introduction

Cardiac ^{123}I-labelled metaiodobenzylguanidine (^{123}I-MIBG) scintigraphy has been suggested to be useful for the diagnosis of idiopathic Parkinson's disease (PD), because many recent studies have revealed that cardiac ^{123}I-MIBG uptake decreases with disease progression and that almost all

patients in the advanced stage of PD show decreased cardiac ^{123}I-MIBG uptake [1–5]. However, it is unclear whether cardiac ^{123}I-MIBG uptake is a good surrogate marker for the diagnosis of PD, especially in early and mild PD cases, which are the most difficult to diagnose in daily clinical practice, because the data on the reduction of cardiac ^{123}I-MIBG uptake in the early stage of PD vary greatly among different studies [1–8]. Therefore, we aimed to investigate the sensitivity and specificity of cardiac ^{123}I-MIBG scintigraphy in diagnosing PD, focusing on early and mild cases of PD in the Hoehn and Yahr (HY) stages 1 and 2.

While planning this study, we focused on dividing the patients into PD and non-PD (NPD) groups in the most appropriate manner in order to acquire precise results. Previous studies have shown that the usual clinical diagnostic accuracy of PD ranges from 70 to 90%, and the accuracy rate greatly decreases in early cases [9–12]. In vivo neurofunctional imaging of the basal ganglia, which provides images of both pre- and postsynaptic nigrostriatal dopaminergic functions, has been recognized as a standard marker for the diagnosis of PD in every clinical stage [13–25]. Therefore, in order to improve the accuracy of the diagnosis of PD, especially in early PD cases, and to classify the patients into the PD and NPD groups in a more appropriate manner, we performed positron emission tomography (PET) imaging with ^{11}C-labelled 2β-carbomethoxy-3β-(4-fluorophenyl)-tropane (^{11}C-CFT) and ^{11}C-raclopride. PET imaging with ^{11}C-CFT and ^{11}C-raclopride can assess the levels of presynaptic dopamine transporter (DAT) and postsynaptic dopamine D_2-like receptor (D_2R), respectively, in the striatum. The two types of PET imaging techniques were together designated as dopamine PET. Further, we proposed the definitions of PD and NPD patterns in dopamine PET findings on the basis of the results which had been confirmed by previous studies.

We also investigated the association between cardiac sympathetic function assessed by cardiac ^{123}I-MIBG uptake, presynaptic nigrostriatal dopaminergic function assessed by striatal ^{11}C-CFT uptake and disease stage determined according to the HY scale.

Materials and methods

Subjects

The present study was a retrospective study. The subjects comprised 39 patients who visited the neurological outpatient clinic at Tokyo Metropolitan Geriatric Hospital from November 2001 to October 2007. They chiefly complained of one or more parkinsonian symptoms, including resting tremor, rigidity, bradykinesia and postural instability. The patients were divided into PD and NPD groups (Fig. 1). Cardiac ^{123}I-MIBG scintigraphy, dopamine PET and magnetic resonance imaging (MRI) were performed for all patients. None of the patients had any concomitant hereditary disorder that could cause parkinsonian symptoms. None of the patients had an individual history of any heart disease. Further, none of the patients were on any medication that could cause parkinsonian symptoms.

For dopamine PET, eight healthy subjects (five men and three women) aged 55–74 years [mean±standard deviation (SD) = 62.3±6.9 years)]were considered as controls. They were deemed healthy based on their medical history, physical and neurological examinations and MRI of the brain. Further, none of them were on medication.

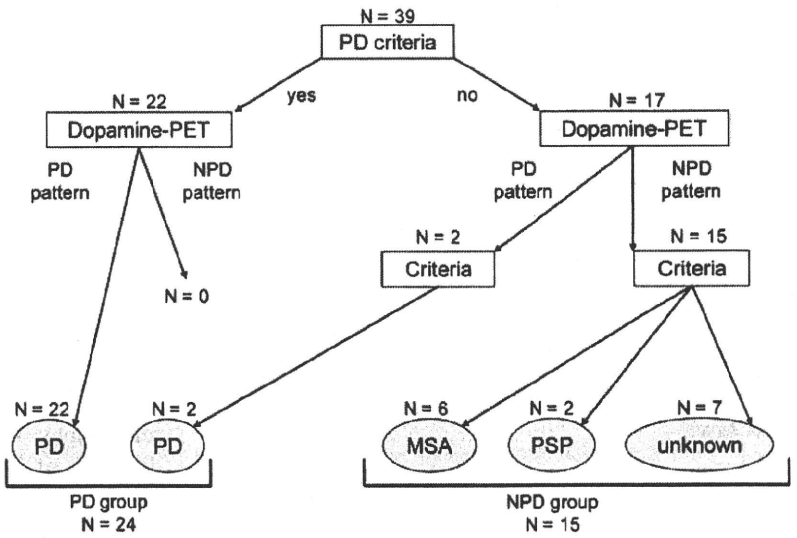

Fig. 1 Diagnostic flow chart and schematic representation of classification process. Patients were classified into PD and NPD groups on the basis of respective published clinical criteria and our dopamine PET findings

This study protocol was approved by the Ethics Committee of the Tokyo Metropolitan Institute of Gerontology. Written informed consent was obtained from all participants.

PET imaging

PET imaging was performed at the Positron Medical Center, Tokyo Metropolitan Institute of Gerontology by using a SET-2400 W scanner (Shimadzu, Kyoto, Japan) in the three-dimensional scanning mode [26], as described previously [27, 28]. The transmission data were acquired using a rotating $^{68}Ga/^{68}Ge$ rod source for attenuation correction. Images of 50 slices were obtained with a resolution of 2×2×3.125 mm voxels and a 128×128 matrix.

Dopamine PET imaging ^{11}C-CFT and ^{11}C-raclopride were prepared as described previously [29, 30]. The two types of PET imaging were performed for all of the subjects on the same day. The patients being treated with antiparkinsonian drugs underwent dopamine PET following at least 15 h deprivation of the medications. Each subject was administered an intravenous bolus injection of 341±62 (mean ± SD) MBq of ^{11}C-CFT, followed by that of 311±56 (mean ± SD) MBq of ^{11}C-raclopride after 2.5–3 h. To measure the uptake of the tracers, static scanning was performed for 75–90 and 40–55 min after the injection of ^{11}C-CFT and ^{11}C-raclopride, respectively. The specific activity of ^{11}C-CFT and ^{11}C-raclopride at the time of injection ranged from 5.9 to 134.2 GBq/μmol and from 10.2 to 201.7 GBq/μmol, respectively.

Analysis of dopamine PET images Image manipulations were performed using Dr. View version R2.0 (AJS, Tokyo, Japan) and SPM2 (Functional Imaging Laboratory, London, UK) implemented in MATLAB version 7.0.1 (The MathWorks, Natick, MA, USA).

The two PET images and one MRI image obtained for each subject were coregistered. The three coregistered images were resliced transaxially, parallel to the anteroposterior intercommissural (AC-PC) line. Circular regions of interest (ROIs) were selected with reference to the brain atlas and individually coregistered MRI images. In each of the three contiguous slices, one ROI with 8-mm diameter was selected on the caudate, two ROIs on the anterior putamen and two on the posterior putamen on both the left and right sides. In other words, the AC-PC plane and regions 3.1 and 6.2 mm above the AC-PC line were selected. A total of 50 ROIs with 10-mm diameter were selected throughout the cerebellar cortex in five contiguous slices.

To evaluate the uptake of ^{11}C-CFT and ^{11}C-raclopride, we calculated the uptake ratio index by the following formula [15, 31]: uptake ratio index = (activity in each region − activity in the cerebellum)/(activity in the cerebellum). We previously validated the method to estimate the binding potential of ^{11}C-raclopride and ^{11}C-CFT, adopting the uptake ratio index [27, 28]. For the further analyses, the uptake of each tracer in each subregion of the striatum (the caudate, anterior putamen and posterior putamen) was evaluated as the average value of the left and right sides. The uptake of each tracer in the whole striatum was evaluated as the average value of entire ROIs in the whole striatum.

Cardiac ^{123}I-MIBG scintigraphy

Scintigraphic studies were performed at Tokyo Metropolitan Geriatric Hospital by using a triple-headed gamma camera (PRISM-3000, Shimadzu, Kyoto, Japan). None of the patients were on any medication, i.e. they were not receiving any drugs such as antidepressants and monoamine oxidase inhibitors, which might influence cardiac ^{123}I-MIBG uptake. After a 30-min resting period, each patient was administered an intravenous bolus injection of 111 MBq of ^{123}I-MIBG (Fujifilm RI Pharma Co., Tokyo, Japan). Planar images of the chest in the anterior view were obtained twice for 5 min, starting at 20 min (early phase) and then at 180 min (delayed phase) after the injection of ^{123}I-MIBG. Relative organ uptake of ^{123}I-MIBG was determined by selecting the ROIs on the heart and mediastinum in the anterior planar image [32]. Average counts per pixel in the heart and mediastinum were used to calculate the heart to mediastinum (H/M) ratio.

MRI

MRI was performed at Tokyo Metropolitan Geriatric Hospital. By using a 1.5-T Signa EXCITE HD scanner (GE, Milwaukee, WI, USA), transaxial T1-weighted images [three-dimensional spoiled gradient-recalled (3D SPGR), repetition time (TR) = 9.2 ms, echo time (TE) = 2.0 ms, matrix size = 256 × 256 × 124, voxel size = 0.94 × 0.94 × 1.3mm] and transaxial T2-weighted images (first spin echo, TR= 3,000 ms, TE=100 ms, matrix size = 256 × 256 × 20, voxel size = 0.7 × 0.7 × 6.5mm) were obtained.

Clinical diagnosis

The diagnostic flow chart is shown in Fig. 1. First, the patients were divided into two groups (22 patients in one group and 17 patients in the other) on the basis of the clinical criteria of the UK Parkinson's Disease Brain Bank (UKPDBB) [10]. Each group was then further classified on the basis of dopamine PET findings. As shown in Fig. 2, the PD pattern in dopamine PET was defined as follows: (1)

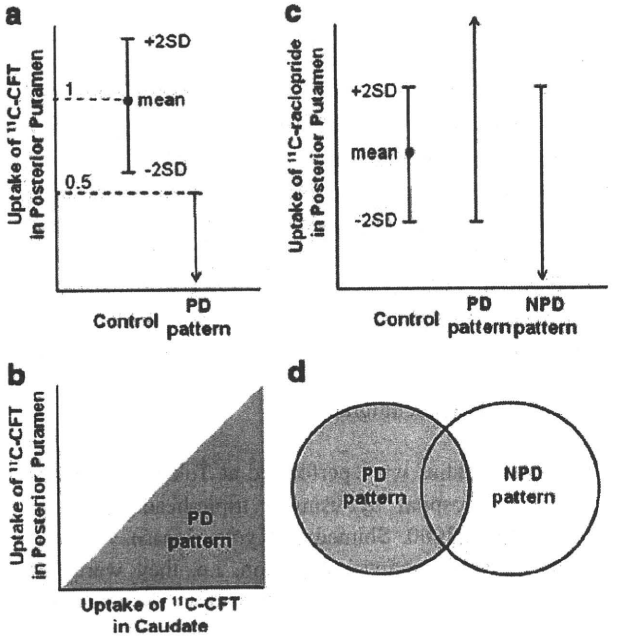

Fig. 2 PD and NPD patterns defined on the basis of dopamine PET findings. PD pattern: ^{11}C-CFT uptake in the posterior putamen of patients less than 50% of the mean uptake in the posterior putamen of normal controls (**a**) and less than that in the caudate of patients (**b**); ^{11}C-raclopride uptake in the posterior putamen of patients more than the mean – 2 SD of the uptake in the posterior putamen of normal controls (**c**). NPD pattern: ^{11}C-raclopride uptake in the posterior putamen of patients less than the mean + 2 SD of the uptake in the posterior putamen of normal controls (**c**). The patient was considered to be PD pattern when both PD and NPD were fulfilled (**d**). The uptake in each subregion of the striatum was evaluated as the average value of both sides

^{11}C-CFT uptake in the posterior putamen of the patients less than 50% of the mean uptake in the posterior putamen of normal controls (Fig. 2a) and less than that in the caudate of the patients (Fig. 2b) and (2) ^{11}C-raclopride uptake in the posterior putamen of the patients more than the mean – 2 SD of the uptake in the posterior putamen of normal controls (Fig. 2c). The NPD pattern was defined as follows: ^{11}C-raclopride uptake in the posterior putamen of the patients less than the mean + 2 SD of the uptake in the posterior putamen of normal controls (Fig. 2c). The patient was considered to be PD pattern when both PD and NPD were fulfilled (Fig. 2d).

Statistical analysis

Differences in the averages and variances were tested by Student's *t* test and one-way analysis of variance, respectively. Correlations between the two groups of patients were assessed by linear regression analysis with Pearson's correlation test; *p* values of <0.05 were considered statistically significant.

Results

Patients

Classification into PD and NPD groups All 22 patients who fulfilled the UKPDBB PD criteria at initial diagnosis [10] showed the PD pattern on dopamine PET (Fig. 1). They were classified into the PD group. The other 17 patients were further classified according to dopamine PET findings and respective published clinical criteria. Of the 17 patients, 2 showed the PD pattern on dopamine PET. In fact, the symptom manifested was only resting tremor at initial diagnosis; however, during the course of the study, they fulfilled the UKPDBB PD criteria [10] and were classified into the PD group.

Of the 17 patients, 15 showed the NPD pattern on dopamine PET and were classified into the NPD group (Fig. 1). These patients were then further divided into three subgroups. Six patients fulfilled the multiple system atrophy (MSA) criteria [33]. Two patients fulfilled the progressive supranuclear palsy (PSP) criteria [34]. For the remaining seven patients, no definitive diagnoses could be established despite follow-up for more than 1 year.

Finally, 24 patients (7 men and 17 women, age range: 60–85 years, mean age ± SD = 71.5±6.8 years) and 15 patients (8 men and 7 women, age range: 65–86 years, mean age ± SD: 76.0±5.5 years) were classified into the PD and NPD groups, respectively.

Demographic data Patient characteristics are summarized in Table 1. In the PD group, 11 patients were drug naive, 7 were being treated with L-dopa and 6 were being treated with L-dopa and dopamine agonists at the time of dopamine PET. The interval between cardiac ^{123}I-MIBG scintigraphy and dopamine PET was within 6 months for 16 patients, between 6 and 12 months for 1 patient and more than 1 year for 7 patients. However, the HY stage of each patient in the PD group remained the same between cardiac ^{123}I-MIBG scintigraphy and dopamine PET. In the NPD group, 11 patients were not administered any antiparkinsonian drug, and 4 were being treated with only L-dopa. The interval between the two examinations was within 6 months for 12 patients, between 6 and 12 months for 1 patient and more than 1 year for 2 patients.

Uptake of ^{123}I-MIBG

Both the early and delayed images showed significantly lower H/M ratios in the PD group than in the NPD group (Fig. 3). In both the early and delayed images, the H/M ratios tended to decrease with the progression of the HY stages; however, the decrease was not statistically significant.

Table 1 Clinical features of patients in Parkinson's disease and non-Parkinson's disease groups

Groups	Patients		Age (years)	Duration (years)	^{123}I-MIBG scintigraphy		^{11}C-CFT PET
	Number	M:F			Heart to mediastinum ratio		Uptake ratio index in the whole striatum
					Early	Delayed	
Parkinson's disease	24	7:17	71.5±6.8	3.5±3.2	1.66±0.45	1.46±0.41	0.98±0.34
Hoehn and Yahr 1	4	0:4	65.0±7.7	2.9±2.6	1.75±0.33	1.49±0.29	1.49±0.40
Hoehn and Yahr 2	9	2:7	73.9±5.6	2.4±1.0	1.81±0.54	1.60±0.45	1.00±0.20
Hoehn and Yahr 3	8	5:3	71.9±7.2	3.0±1.8	1.57±0.44	1.41±0.44	0.81±0.20
Hoehn and Yahr 4	3	0:3	72.3±5.0	9.0±6.1	1.36±0.05	1.12±0.08	0.69±0.07
Non-Parkinson's disease	15	8:7	76.0±5.5	2.8±1.9	2.35±0.46	2.18±0.51	1.65±0.68

Data are expressed as mean±SD

Table 2 shows the sensitivity and specificity of cardiac ^{123}I-MIBG scintigraphy in differentiating patients with PD from the other patients with chief complaints of parkinsonian symptoms. When the optimal cut-off levels of ^{123}I-MIBG were set at 1.95 and 1.60 by receiver-operating characteristic analysis, the sensitivity of cardiac ^{123}I-MIBG scintigraphy for the diagnosis of PD was 79.2 and 70.8% and the specificity was 93.3 and 93.3% in the early image and delayed images, respectively. In HY 1 and 2 PD patients the sensitivity was 69.2 and 53.9% and in HY 3 and 4 PD patients the sensitivity was 90.9 and 90.9% in the early image and delayed images, respectively

Uptake of ^{11}C-CFT

The uptake of ^{11}C-CFT in the whole striatum decreased with the progression of the HY stages (Fig. 4). Significant reduction in the ^{11}C-CFT uptake with the progression of the HY stages was also observed in each of the three subregions of the striatum. Correlation between cardiac ^{123}I-MIBG scintigraphy and ^{11}C-CFT PET was evaluated in the 16 patients who underwent the two examinations within 6 months. There was no significant correlation between the ^{11}C-CFT uptake in the whole striatum and the H/M ratios in both the early images (r=0.15, p=0.59) and delayed images (r=0.21, p=0.43) (Fig. 5). Further, no significant correlation was observed between the ^{11}C-CFT uptake in each of the three subregions of the striatum and the H/M ratio.

Discussion

In the present study, we investigated the sensitivity and specificity of cardiac ^{123}I-MIBG scintigraphy in diagnosing PD and differentiating the patients with PD from the others with chief complaints of parkinsonian symptoms. Further, we investigated the correlation between cardiac sympathetic function assessed by cardiac ^{123}I-MIBG uptake, nigrostriatal

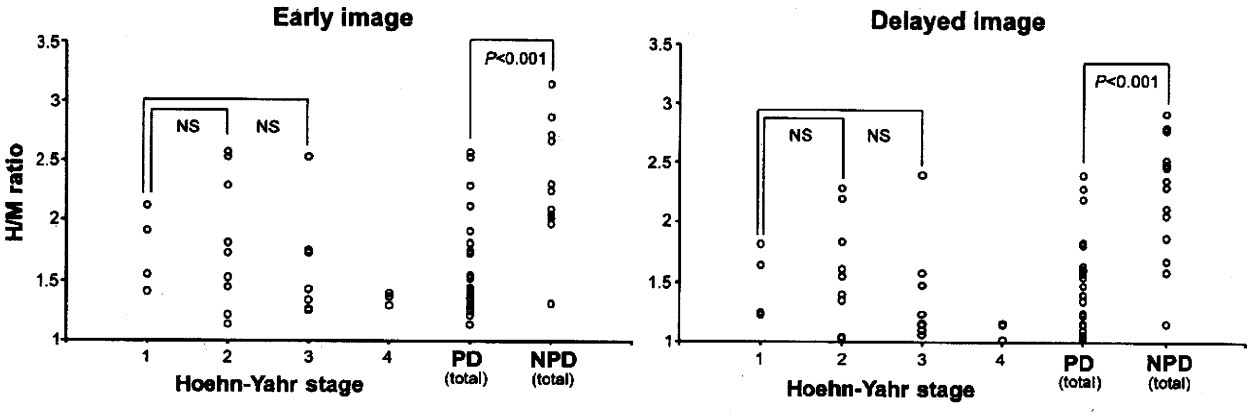

Fig. 3 H/M ratios in the PD and NPD groups in early and delayed images. Each graph represents the relation between the H/M ratio and Hoehn and Yahr stage of PD and a comparison of the H/M ratios of the total number of PD and NPD patients. Both images showed that the H/M ratios were significantly lower in the PD group than in the NPD group; however, the H/M ratios of patients in HY 1 of PD were not significantly higher than those of the patients in HY 2 and 3 of PD. *NS* not significant